Noncovalent nanoarchitectures on surfaces: from 2D to 3D nanostructures

Olga Crespo-Biel,[a] Bart Jan Ravoo,[a] David N. Reinhoudt[a] and Jurriaan Huskens*[ab]

Received 22nd June 2006, Accepted 26th July 2006
First published as an Advance Article on the web 14th August 2006
DOI: 10.1039/b608858a

Nanofabrication requires new methodologies for the assembly of molecular to micrometre-scale objects onto substrates in predetermined arrangements for the fabrication of two and three-dimensional nanostructures. The positioning and the organization of such structures into spatially well-defined arrays constitute a powerful strategy for the creation of materials structured at the molecular level, and to extend the desired properties of these materials to the macroscopic level. Self-assembly is the pathway that enables the formation of such structures, and the formation of multiple supramolecular interactions is the key to controlling the thermodynamics and kinetics of such assemblies. This article is devoted to some representative examples to assemble molecules and nanoparticles in solution and at surfaces based on noncovalent interactions as a tool for the construction of two and three-dimensional systems.

1. Introduction

Molecular self-assembly is the spontaneous association of molecules under equilibrium conditions into stable, structurally well-defined aggregates joined by noncovalent interactions. Self-assembly based on selective control of noncovalent interactions provides a powerful tool for the creation of structured systems at a molecular level, and application of this methodology to molecular systems provides a means for extending such structures to macroscopic lengthscales. Therefore, molecular self-assembly has appeared as a useful tool for the fabrication of materials with characteristic lengthscales of 1–100 nm, thus facilitating the chemical "bottom-up" approach.[1] A single, ordered layer of molecules anchored on a surface can be used as a platform because, in principle, its orientation and positioning can be controlled, producing well-defined structural motifs organized over large areas in two dimensions (2D), or volumes in three dimensions (3D). Self-assembled monolayers (SAMs)[2] are ordered molecular assemblies formed by the adsorption of an adsorbate on a solid surface. The order of these SAMs relies on the spontaneous chemisorption at the interface, as the system approaches equilibrium. A considerable number of self-assembling systems have been investigated in recent years, both on flat substrates[3] and on nanoparticle surfaces.[4] The versatility and flexibility, both at individual molecular and at materials levels, make SAMs valuable substrates for the investigation of specific interactions at interfaces and platforms for the production of 2D and 3D assemblies.[5,6]

Multivalent interactions involve the simultaneous binding of multiple ligand sites on one entity to multiple receptor sites on

[a]*Laboratories for Supramolecular Chemistry & Technology and Molecular Nanofabrication, MESA+ Institute for Nanotechnology, University of Twente, P.O. Box 217, 7500 AE, Enschede, The Netherlands*
[b]*Strategic Research Orientation "Nanofabrication", MESA+ Institute for Nanotechnology, University of Twente, P.O. Box 217, 7500 AE, Enschede, The Netherlands. E-mail: j.huskens@utwente.nl*

Olga Crespo Biel

Olga Crespo Biel (1978) studied chemistry at the Universitat Autònoma de Barcelona (Spain) from 1996 until 2001. From October 2000 to March 2001 she was an Erasmus student in the group of Catalytic Processes and Materials at the University of Twente. In November 2001 she returned to Twente and joined the Supramolecular Chemistry and Technology group directed by Prof. D. N. Reinhoudt, where she worked as a PhD student under the supervision of Prof. J. Huskens and Dr. B. J. Ravoo. At present she is working as a postdoctoral researcher in department of Performance Materials Chemistry and Technology at DSM Research (The Netherlands).

Bart Jan Ravoo

Bart Jan Ravoo (1970) obtained his graduate and postgraduate degrees in chemistry from the University of Groningen, The Netherlands. In 1999 he moved to University College Dublin, Ireland where he held a Newman Scholarship for a period of three years. In 2002 he was appointed as assistant professor at the University of Twente. His main research interest is self-assembly and molecular recognition in water and at the dynamic interface between water and (soft) surfaces. His research includes the development of functional SAMs, soft lithography and nanofabrication.

another, and can result in the formation of numerous simultaneous complexes that afford a high functional affinity.[7] The selectivity and the number of interactions involved in the binding of multivalent species makes multivalency useful for creating stable and complex molecular assemblies. Thus, multivalency has started to emerge as a powerful self-assembly tool in supramolecular chemistry and in nanofabrication schemes.[8]

Nanotechnology requires new methodologies for the assembly of molecular to micrometre-scale objects onto substrates in predetermined arrangements for the fabrication of 3D nanostructures. Such nanostructures will have controllable sizes in all three directions. However, self-assembly by itself is still unable to produce such devices and so top-down surface patterning methods, such as soft lithography, are required. The combination of a top-down surface patterning method, to achieve x, y control, with a self-assembly method to tune the z direction will lead to well-defined, high-resolution 3D nanostructures of a large variety of materials.

The first part of this review highlights examples of self-assembled systems in which complementary recognition functionalities are arranged in a 2D plane, and demonstrates how these systems can be employed towards the construction of multilayered 3D nanostructures. The second part is devoted to examples of 3D assemblies where the recognition motif is anchored on a nanoparticle surface, and the multivalent binding events result in the controlled aggregation of these nanoparticles.

2. Self-assembled nanoarchitectures on 2D and 3D surfaces

One of the key challenges in nanofabrication is the positioning of individual units, such as small molecular ligands, larger molecules, proteins and nanoparticles with nanometre precision. Supramolecular interactions, such as those observed in host–guest complexes, are specific and directional, and a wealth of information is usually available on their binding strengths and kinetics. Moreover, the application of molecules that allow the formation of multiple supramolecular interactions provides a tool to tune adsorption and desorption because the thermodynamic and kinetic parameters are related to the number of interactions, and the strength and kinetics of an individual interaction.

This section is devoted to different systems and methodologies that have been used in order to attach molecules and nanoparticles onto surfaces through specific and selective noncovalent interactions. Moreover, some examples of layer-by-layer systems will be described as a potential platform for the construction of three-dimensional (3D) systems.

2.1 Self-assembly of molecules on SAMs

There are many examples in the literature of molecular recognition of small molecules on SAMs formed from complex synthetic receptors, such as cyclodextrins and calix[n]arene derivatives. These ''hosts'' contain a molecular cavity for the recognition of ''guest'' molecules. The challenge has been to understand the role of molecular structure, organization, and interactions in the recognition process and thereby improving selectivity. Therefore, a detailed understanding of molecular recognition of small molecules at interfaces is required.

Calix[n]arene-based adsorbates were shown to give well-packed, ordered monolayers[9,10] capable of interacting with small guests such as tetrachloroethylene and toluene in the vapor phase,[11] and steroids[12] or other neutral molecules[13,14] in aqueous solution. In a recent study, Gupta and co-workers demonstrated that thiolated calix[4]arene molecules assembled on gold surfaces could discriminate between two structural isomers. The authors postulated that the combination of factors such as hydrogen bonding, hydrophobic interactions and steric match permitted such discrimination.[15]

Cyclodextrins (CDs) constitute a different type of receptor molecule. They contain hydrophobic cavities lined by the glycosidic oxygen bonds, which are responsible for the ability of CDs to include hydrophobic molecules. Such a hydrophobic cavity makes them ideal hosts for molecular recognition in aqueous solution.[16] Several routes for the immobilization of

David N. Reinhoudt

David N. Reinhoudt was born in 1942 in The Netherlands and obtained a PhD in chemistry in Delft in 1969. From 1970 to 1975 he worked at Shell on the crown ether research program. He was appointed as a part-time professor at the University of Twente in 1975 and as a full professor in 1978. Nowadays he is in charge of the Laboratory of Supramolecular Chemistry and Technology, scientific director of the MESA+ Institute for Nanotechnology, and chairman of the Board of NanoNed, the Dutch program for Nanotechnology. He is the author of more than 800 scientific publications and patents.

Jurriaan Huskens

Jurriaan Huskens (1968) studied chemical engineering at the Eindhoven University of Technology and obtained his PhD from the Delft University of Technology in 1994. In 1995 and 1996, he was a postdoc with Prof. Sherry at the University of Texas at Dallas, USA. In 1997, he was awarded a Marie Curie fellowship to work in the group of Prof. Reetz at the Max-Planck-Institut für Kohlenforschung, Mülheim an der Ruhr, Germany. In 1998, he became an assistant professor in the group of Prof. Reinhoudt. In 2005 he was appointed as program director ''NanoFabrication'' of the MESA+ Institute for Nanotechnology and soon after as full professor of Molecular Nanofabrication at the University of Twente.

cyclodextrins on surfaces have been developed, mainly on gold[17] and recently on other types of surfaces such as silicon oxide.[18] The most common CD SAMs are prepared from *per*-6-functionalized cyclodextrins, first reported by Kaifer *et al.* in 1995,[19] in which the CD cavities are immobilized upwards with their secondary face towards the solution readily available for complexation of guest molecules. Binding studies at such SAMs have been performed with a variety of small hydrophobic guest molecules. Ferrocene derivatives,[19,20] dopamine,[21] coumarin,[22] azo compounds[23,24] steroids,[25] phenyls,[23,25] adamantyls,[25] bisphenols,[26] and charged guests[27,28] among others, have been studied by means of surface plasmon resonance (SPR) spectroscopy, electrochemical methods, Raman spectroscopy, and single molecule force spectroscopy. In the last method, the rupture force of an individual host–guest complex is determined by pulling a guest-modified AFM tip off the host SAM.[29] Thus, CDs on surfaces are suitable host molecules showing similar binding properties as in solution. Since CDs are chiral, it is also possible for CDs to recognize the chirality of guest molecules. The group of Kitano *et al.* took advantage of the chiral recognition properties of CDs and investigated the regio- and stereoselective complexation of optically active azo dyes, showing that the enantioselectivity of CD was preserved after immobilization onto a solid surface.[24]

In our group, a wide range of molecules (calix[4]arenes, dendritic wedges and dendrimers) functionalized with multiple adamantyl and ferrocenyl units have been immobilized onto CD SAMs on gold and silicon oxide surfaces.[30–34] Stable positioning and patterning of such molecules was achieved by means of multivalent supramolecular interactions between the hydrophobic moieties at the guest molecules and the CD cavities at the surface. These host surfaces serve as ''molecular printboards'' for the positioning of guest molecules.[31,33] Besides developing a thermodynamic model for studying the interactions at interfaces,[35] our group has also been able to determine experimentally the number of interactions of these hydrophobically modified molecules towards the CD SAM, enabling the tuning of adsorption and desorption processes at surfaces using the number of interactions.[33,34] Moreover, it has been possible to electrochemically induce desorption at CD SAMs by using ferrocene-terminated dendrimers, revealing the possibility to intentionally adsorb and desorb molecules to and from surfaces (Fig. 1A).[36] Furthermore, molecular patterns of guest-functionalized calix[n]arene molecules, dendritic wedges labeled with fluorescent groups, and dendrimers have been prepared on these molecular printboards by using the readily accessible (soft) lithographic techniques such as microcontact printing (μCP) and dip-pen nanolithography (DPN).[31,32,37]

Myles and co-workers have described the immobilization of barbituric acid derivatives on mixed monolayers of alkanethiols and bis(2,6-diaminopyridine) amide of isophthalic acid-functionalized decanethiol on gold films. The immobilization of the barbiturate derivatives to the receptor-functionalized SAM involved the use of multiple hydrogen bonds to achieve a stable assembly on the surface, showing equal 1 : 1 stoichiometry in solution and on surfaces.[38] A more complex system, also involving barbituric acid derivatives, was reported by our group where individual synthetic hydrogen-bonded assemblies were grown on SAMs on gold surfaces.[39] The approach used is based on the spontaneous formation of stable hydrogen-bonded assemblies in apolar solvents between calix[4]arene dimelamines and barbituric/cyanuric acid derivatives, where 9 molecules are held together by 36 hydrogen bonds. The growth of the assemblies at the surface was performed by embedding the thioether-modified calix[4]arene dimelamines into a thiolate SAM. Subsequently, the monolayers containing one of the building blocks were immersed in a solution of the already formed hydrogen-bonded assembly, resulting in stable hydrogen-bonded assemblies at the surface.

Functionalized nanotubes, which can recognize specific complementary molecules, have become increasingly important in the design of nanometre-sized functional materials. The group of Matsui *et al.* functionalized a peptide nanotube, which specifically and selectively binds a well-defined region on a complementary ligand-patterned substrate. They have employed azobenzene[40] and ferrocene[41] groups as a linking unit for the immobilization of nanotubes at CD SAMs on gold surfaces. Hydrogen bonding interactions between the hydroxyazobenzenecarboxylic acid and the amide functionalities on the *trans*-form of the azobenzene moieties were employed to assemble the azobenzene-functionalized peptide nanotubes onto α-CD SAMs in an ethanol–water mixture. Upon UV-irradiation, the azobenzene moieties switched to the *cis*-form, which has a lower affinity for α-cyclodextrin, and thus resulted in desorption of the nanotubes from the surface (Fig. 1D).[40] In the case of the ferrocene-functionalized peptide nanotubes, desorption from a β-CD SAM took place by tuning electrochemically the redox states of ferrocene moieties.[41] Only in the latter case, control experiments were performed on α-CD SAMs showing the size specificity of the host–guest recognition of the ferrocene-nanotubes towards the β-CD SAM. In another example, molecular nanotubes formed by the one-dimensional linkages of α-CDs, were immobilized through a monovalent inclusion complex formation with dodecanethiol onto self-assembled monolayers of inclusion complexes between dodecanethiol and β-CD. Surface plasmon resonance (SPR) measurements showed a lower thickness of the molecular tubes after immobilization, which can be related to a partial adsorption or domain formation of the molecular tubes on the dodecanethiol-β-CD SAM.[42]

Polymers tethered onto surfaces have been subject of attention owing to their potential use in many surface-based devices and technologies such as switchable membranes, sensors, cell growth, and biomimetic materials.[45–48] Some examples of polymers modified with molecular recognition sites assembled onto functionalized SAMs with complementary sites have been described. A study of particular interest by Whitesides and co-workers employed a bifunctional polymer presenting vancomycin (Van) and fluorescein groups for the detection of anti-fluorescein antibodies to SAMs containing D-alanine-D-alanine (DADA) moieties.[49] These polymers were shown to bind specifically to these SAMs *via* multiple interactions between DADA and Van groups. SPR was used to study the binding of the polymer to the SAM and, subsequently, the binding of antibodies to the surface comprising the SAM and a film of adsorbed polymer. The SPR sensograms showed the strong adsorption of the bifunctional

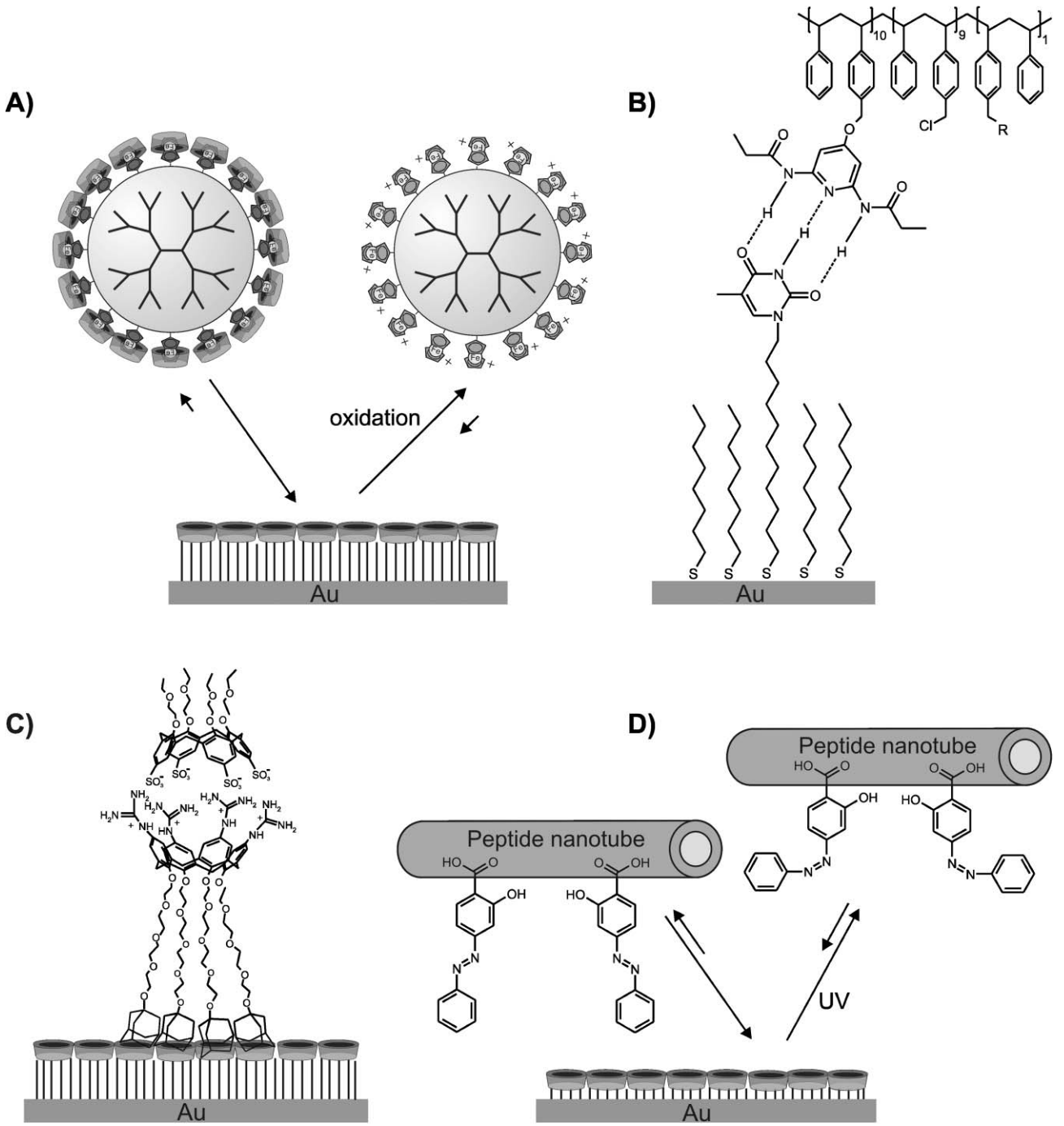

Fig. 1 Molecules on SAMs: electrochemically induced desorption at CD SAMs by using ferrocene-terminated dendrimers (A),[36] polymers tethered to surfaces using hydrogen bond interactions (B),[43] positioning of molecular capsules at CD SAMs (C),[44] and attachment of peptide nanotubes on CD SAMs (D).[40]

polymer to the SAM due to the multiple interactions available for binding. Desorption was possible by adding a competitor in solution, while inhibition of binding between the anti-fluorescein antibody and the polymer tethered on the surface was achieved by using a soluble fluorescein derivative.

We have studied the molecular recognition by CD SAMs of poly(isobutene-*alt*-maleic acid)s modified with hydrophobic *p*-*tert*-butylphenyl or adamantyl groups.[50] The multivalent binding of the guest polymers with the CD SAMs were investigated as a function of the nature and number of hydrophobic groups that interact with the CD surface and the intramolecular interactions within the polymer. The interaction is driven by the multiple inclusion complexes formed between the polymer guest and the CD surface. The adsorption was shown to be strong, specific and irreversible, where the polymer adsorbed onto the CD surface as a very thin layer employing efficiently all or most of the hydrophobic groups. Even competition with a monovalent host or guest in solution

did not lead to measurable polymer desorption. This behavior could be attributed to the large number of hydrophobic groups present in the polymer and to the close-to-optimal linker lengths between the hydrophobic groups relative to the periodicity of the CD lattice.[35,51]

Rotello and co-workers used complementary three-point hydrogen-bonding interactions between modified SAMs and complementary functionalized mono- and di-block copolymers to direct the adsorption process onto surfaces.[43,52,53] The thymine-diamidopyridine (Thy-DAP) hydrogen-bonding motif provided a highly selective adsorption of the DAP-containing mono- and di-block copolymers onto the Thy-decorated gold surface under controlled deposition conditions. In spite of the multiple binding moieties, desorption of the polymer from the surface could be induced by increasing polarity of the solvent and by rising the temperature, due to the nature of the hydrogen-bonding interactions, and thus creating renewable surfaces (Fig. 1B). Using similar hydrogen-bonding interactions, the group of Yoon and co-workers were able to organize microcrystals on glass consisting of thymine and 3-methylthymine modified-zeolite crystals tethered on an adenine-modified glass surface.[54]

An interesting supramolecular assembly on flat surfaces towards the construction of 3D nanostructures is the assembly of supramolecular containers on functionalized SAMs. The group of Shinkai reported the formation and subsequent immobilization of a hexacationic homooxacalix[3]arene-[60]fullerene 2 : 1 complex on anion-coated SAMs on gold and studied their photoelectrochemical response under UV-irradiation.[55] Our group reported the formation of a resorcin[4]arene–based carceplex onto a SAM on gold,[56] and the formation of a molecular cage based on metal–ligand coordination at surfaces, with one of the components directly anchored to a gold surface.[57,58] Furthermore, our group also reported the stepwise formation of a supramolecular capsule on the surface by using the noncovalent attachment of one component of the molecular capsule onto a β-CD SAM followed by the electrostatic self-assembly of the second component at the interface (Fig. 1C).[44] The positioning and the stepwise assembly of the molecular capsule on the surface was monitored by SPR, showing a 1 : 1 complex with an association constant comparable to the complex in solution ($7.5 \times 10^5\ M^{-1}$). The stable binding of one of the components onto the surface, ensured by multiple host–guest interactions, enabled the reversible capsule formation in two steps: first the disruption of the electrostatic interactions, and in a second step of the host–guest interactions.

2.2 Self-assembly of nanoparticles on SAMs

Particles typically ranging in size from 1 nm to several μm play a major role in the development of nanoscience and nanotechnology.[59] Nanoparticles (NPs) are promising candidates for the construction of new nanomaterials. The controlled organization and precise positioning of NPs on 2D surfaces, as well as their hierarchical self-organization, are essential for the development of new functional materials that can be applied in numerous sensing, electronic, optoelectronic, and photoelectronic applications.[60]

A variety of methodologies such as colloidal epitaxy, capillary forces, the application of an external electric field, or covalent attachment have been employed to induce NP self-assembly on surfaces.[61] However, this section will be devoted to an overview of different examples of immobilization of NPs on chemically-modified solid supports, where colloidal self-assembly takes place *via* specific noncovalent interactions. Some weak interactions to form ordered 2D particle arrays will be discussed followed by the use of biological molecules and their molecular recognition properties to guide the assembly.

Among the different immobilization approaches, electrostatic self-assembly has been most widely used to direct NP assembly on surfaces. Electrostatic forces, which are mediated by a protective organic layer and by a linker molecule, are strong enough to ensure a sufficient stability of the assembly, but nevertheless weak enough to allow a reaction of the system to environmental changes, such as ionic strength or pH.[62,63]

An example of electrostatic assembly of NPs on solid supports involves the interaction between positively charged amino groups and negatively charged carboxylate groups. For example, the group of Auer *et al.* studied the formation of gold NP assemblies on planar gold surfaces modified with mercaptohexadecanoic acid using bis-benzamidines as a linker group between two negatively charged gold surfaces.[64] In this three-step process, the different quality and order on the bis-benzamidine linker resulted in variations of the layer thickness and density of the charged NPs. The versatility of the electrostatic assembly has been applied in other systems such as the assembly of silver NPs[65] and gold nanorods.[66] This protocol requires the formation of a SAM on a substrate, followed by immersion of the substrate in a colloidal solution. The first step determines the surface coverage of NPs at the surface.[67] Adsorption of particles by this method results in only monolayer and submonolayer coverages since further adsorption on the surface is prevented by electrostatic repulsion between the charged particles.

The group of Maoz and Sagiv developed a versatile self-assembly approach for the *in-situ* chemical surface generation of spatially defined nanostructures, based on a non-destructive patterning process that allows the further functionalization on the surface of a highly ordered long-tail organosilane SAM on silicon oxide (Fig. 2).[68,69] The approach, called "constructive nanolithography", is based on applying an electrical bias to a conducting AFM tip to induce an electrochemical surface transformation affecting the outer exposed functional groups of a SAM, while preserving the overall monolayer structural integrity. The AFM tip induces oxidation of the surface-exposed vinyl[68] and methyl[69] groups to hydroxyl-containing functionalities, which can participate in further self-assembly and chemical modification. Particularly, this method has been employed to produce organic film patterns (monolayers and thicker layered assemblies) for precise control of the self-assembly pattern of selected inorganic materials such as metals and semiconductors (CdS).[70] This methodology was also applied in different routes for the template-guided assembly of gold NPs.[71,72] Synthesized Au_{55} clusters were successfully organized *ex-situ* by guided self-assembly on such tip-modified bilayer template patterns, by ligand exchange mechanism of the Au_{55} to the thiolated surface sites.[71] In a

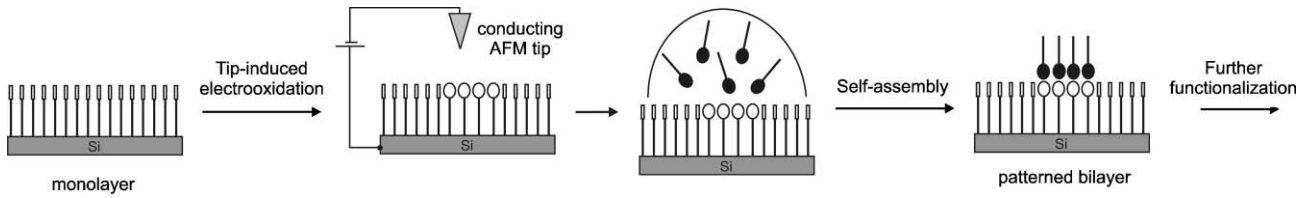

Fig. 2 Schematic representation of constructive nanolithography as a generic method for the directed self-assembly of nanostructures on surfaces.[68,69]

different route, negatively charged gold NPs were self-assembled on positively charged bilayer template patterns with top amino functionalities.[72]

The group of Schubert utilized the constructive nanolithography approach for the controlled assembly of differently sized particles to a surface. The tip-modified surface exhibited negatively charged carboxylate groups, that were used as templates for the site-selective binding of cationic gold NPs and amine-terminated CdSe–ZnS core–shell NPs.[73] In this approach the first tip-induced oxidation allowed the first assembly of particles, while the application of a second oxidation step in close proximity to the already present NPs, resulted in complex nanostructures decorated with a range of different NPs. The same procedure was applied in the fabrication of nanosized magnetic structures.[74]

Polymers tethered on surfaces have also been used as a template for ordering nanoparticles through multiple electrostatic interactions. Miyashita and co-workers employed polymer nanosheets, which were transferred onto a solid support by the Langmuir–Blodgett method, where negatively charged gold NPs could be adsorbed effectively onto the positively charged polymer nanosheet containing 4-vinyl-pyridine, yielding an adsorbed gold NP monolayer.[75] In addition, a patterned gold NP monolayer was obtained with photopatterned polymer nanosheets. In another approach using polymers for NP assembly, Bhat *et al.* described the use of surface-bounded polymer brushes to create different density gradients of NPs depending on the polymer chain length (Fig. 3).[76] Polyelectrolytes have also been used to assemble NPs on surfaces in a multilayer fashion using the well-known layer-by-layer (LBL) technique (Section 2.3).

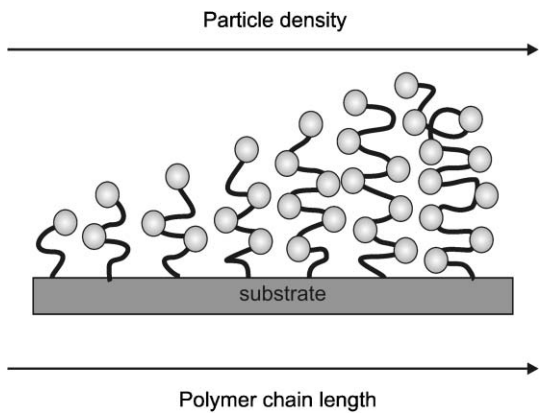

Fig. 3 Schematic drawing representing the spatial distribution of dispersed gold NPs adsorbed along a surface-anchored poly(acryl amide) brush with a molecular weight gradient.[76]

To advance from micro- to nanometre-sized patterns, our group used nanoimprint lithography (NIL) to create NIL-patterned SAM substrates to electrostatically direct NP adsorption.[77] In this case the endgroup functionality of the NIL-patterned SAM was used to direct the deposition of functionalized particles. NP deposition was achieved on samples where the polymer was still present or on samples where a second SAM was assembled after polymer removal. This second SAM can be used to tune the selectivity for NP adsorption.

Related approaches for the immobilization of NPs using hydrophobic interactions have also been described. A straightforward mechanism was described by Dong and co-workers where two different kinds of hydrophobic surfaces promoted NP assembly.[78] Hydrophobically-modified NPs were assembled on two different kinds of hydrophobic surfaces, 1-decanethiol (DT) and 2-mercapto-3-*n*-octylthiophene (MOT). The NPs showed a higher affinity for the MOT SAM compared to the DT SAM, which was attributed to an enhanced hydrophobic effect due to a more loosely packed MOT monolayer.

A more sophisticated approach to immobilize NPs on solid supports was developed by Fitzmaurice and co-workers by using a pseudorotaxane formation between an electron-rich crown ether (dibenzocrown-8) and an electron-poor cation (dibenzyl-ammonium) as the driving force for the assembly.[79] They prepared a silicon wafer modified with the precursor of the dibenzylammonium cation moiety. The cation precursor was converted to the corresponding cation by exposure to blue light. After immersion of the substrate in a solution containing the crown-modified NPs, SEM images showed that these NPs were adsorbed predominantly at the cation-modified regions.

Our group exploited the multiple hydrophobic interactions presented between adamantyl-terminated poly(propyleneimine) (PPI) dendrimers and cyclodextrin-modified silica NPs to create stable and dense monolayers of these particles onto a cyclodextrin surface. Control experiments with glucosamine-functionalized silica particles resulted in a very low coverage, thus confirming the supramolecular specificity needed for efficient adsorption.[80]

Recently, Binder and co-workers developed a new methodology for NP immobilization on flat surfaces through specific hydrogen bonding interactions.[81] They based their approach on the multiple hydrogen bonding interactions of the "Hamilton-type" receptor (Fig. 4). Two gold NP sizes were used in the study, 5 and 20 nm respectively. It was found that the surface coverage of NPs could be adjusted by the receptor in the mixed SAM. Additionally, the authors estimated the number of receptor molecules that could participate in the NP

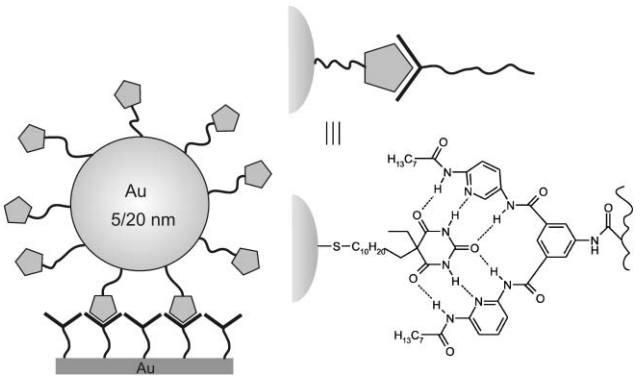

Fig. 4 Concept of NP binding mediated by the "Hamilton-type" receptor.[81]

binding to 45 for the 20 nm NPs and 3–4 for the 5 nm NPs. The stability of the NP assembly was proven by repetitive imaging of the same area, whereas the specificity of the assembly was established by the absence of binding of octadecyl-modified gold NPs to the receptor-modified surface.

The immobilization of biomolecule–nanoparticle hybrid systems on surfaces provides unique features for the generation of ordered NPs arrays. Biomaterials, such as nucleic acids, streptavidin–biotin, or antigen–antibody complexes provide interesting templates for the immobilization of NPs. Additionally, hybrid biomolecule–NP composites on surfaces provide functional interfaces that can be employed for sensor, photoelectrochemical, and electronic circuitry applications.[82] However, these subjects will not be discussed in this section because they have been reviewed by others.[82,83] Nucleic acids can serve as templates to bind DNA-functionalized nanoparticles at complementary segments. When DNA templates are fixed at a surface of a solid support, the resulting assemblies of NPs can yield a pattern that is dependent on either the shape produced by the DNA template itself or on the pattern produced upon its immobilization.

Niemeyer and co-workers prepared oligofunctionalized gold NPs containing different DNA sequences and varying the number of DNA sequences attached to the NPs, ranging from one up to seven.[84] Biotinylated oligomers were immobilized on streptavidin-coated microplates, and saturated with complementary linker oligonucleotides providing the specific sequence complementary to the gold particle-bound oligonucleotides (Fig. 5). Hybridization of the complementary oligonucleotide sequences, resulted in the immobilization of DNA-gold NPs, and furthermore led to the formation of a silver precipitate that was quantified by absorbance measurements. In a following study, gold NPs functionalized with two different oligonucleotides were used as building blocks that contained two independently addressable DNA sequences: one of the sequences was utilized for attaching the gold NPs at the solid support, while the other sequence was used to establish lateral crosslinks between the adjacently immobilized NPs.[85] A similar approach was applied by Mirkin *et al.* to construct mono- and multilayered DNA-gold NP structures on a glass support.[86] In another study, Niemeyer and co-workers used the linkage of an antibody–antigen complex to create NP assemblies.[87]

Self-assembly of metallic NPs into high density 2D arrays has been obtained by a process in which DNA–gold NPs were hybridized to a pre-assembled 2D DNA scaffold deposited onto a mica surface.[88] The latter was designed to form rows of hybridization sites with a 4 nm spacing between sites and a 64 nm separation between rows. The DNA–gold NPs functionalized with multiple complementary DNA strands were hybridized to the pre-assembled 2D DNA scaffold. AFM images of samples taken after the NP hybridization step

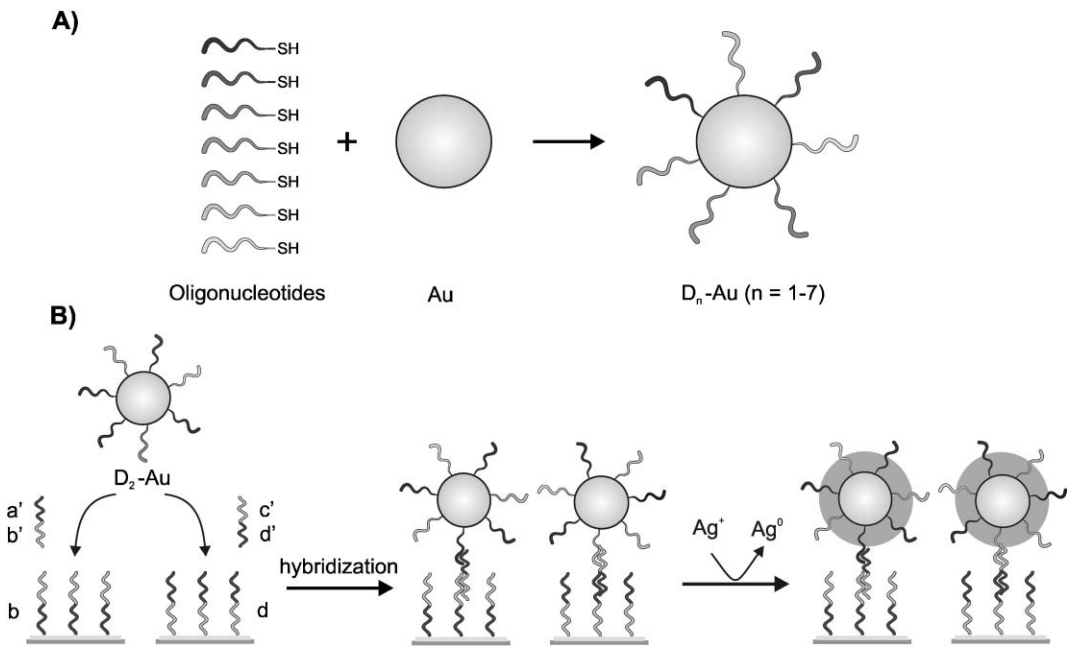

Fig. 5 (A) Schematic drawing of the preparation of the oligofunctionalized DNA–gold NPs (D_n–Au) containing different DNA sequences. (B) DNA-directed immobilization of D_2–Au and subsequent silver enhancement step.[84]

revealed an assembly of closely-packed particles along the lines on the scaffold. This methodology could be interesting for the assembly of 2D nanoelectronic components arrays and their further application in nanodevices and circuits. Similar approaches based on DNA-hybridization driven self-assembly have been used for the immobilization of nanowires.[89]

Another approach to the directed placement of NPs on solid supports by means of DNA hybridization is based on the micro- and nanopatterning of a surface with DNA molecules followed by hybridization with complementary-DNA functionalized NPs. This approach provides the specific immobilization of NPs at target domains of the pattern. Micropatterns of DNA-functionalized NPs were obtained by depositing an amine derivative of an oligonucleotide in a pattern onto a chemically modified glass surface using a nanoliter dispensing device. Gold NP patterns were formed by hybridization of the patterned DNA regions with the complementary DNA-modified NPs.[90] A more direct and precise placement of gold NPs was demonstrated by dip-pen nanolithography (DPN), which was applied to the patterning of the primary DNA on the surface followed by hybridization with complementary DNA-functionalized NPs.[91,92] A similar approach was used to pattern surfaces with functionalized gold NPs by DPN based on antigen-antibody interactions.[93]

3 Multilayer thin films

3.1 General aspects of layer-by-layer assembly

In the previous sections, several methodologies to assemble monolayers ranging from small to larger molecules such as polymers and nanoparticles have been discussed. These approaches can be extended to multilayer films that can enhance the properties of monomolecular films and at the same time create a new class of materials possessing functional groups at controlled sites in three-dimensional arrangements. Such structures require control of molecular orientation and organization at the nanometre scale, and therefore it is essential to study and develop methods for the controlled assembly of multicomponent nanostructures.

Layer-by-layer (LBL) assembly[94] has emerged as a promising method for fabricating structured and functional thin films on solid supports. LBL assembly is an approach based on the alternate adsorption of materials containing complementary charged or functional groups to form multicomponent ultrathin films as illustrated schematically in Fig. 6. LBL assembly has been defined as a versatile, universal and simple method to assemble building blocks of different compositions into ultrathin multilayer films with controlled thickness and molecular structure on arbitrary solid substrates. Some interesting properties and possible applications of LBL films will be discussed in this section. The references hereby described are intended only to give some introductory information about selected recent developments of LBL assembly, which has been well covered by recent books and reviews.[95,96]

The LBL method has been most often manifested in the alternation of oppositely charged species.[96] However, it has been successfully extended to various other driving forces such as hydrogen-bonding,[97] charge transfer,[98] acid base pairs,[99] metal–ion coordination,[100] inter- or intramolecular interactions in the dried state,[101] covalent bonds,[102] biospecific interactions (*e.g.* sugar–lectin interactions),[103] and host–guest interactions between cyclodextrin dimers and ferrocene-appended poly(allylamine) polymers[104]. In general, one can use any interaction (this may be one or several different types of interaction) between two species in order to incorporate them into a multilayer film. For example, Rubner and co-workers introduced for the first time hydrogen-bonding interactions between two conjugated polymers as a driving force for LBL assembly.[97] The LBL assembly was demonstrated with polyaniline, which can form strong hydrogen bonds at both the amine and imine sites along its polymer backbone, and a variety of different nonionic water-soluble polymers. Rubinstein and co-workers described the use of coordination chemistry in the multilayer assembly on gold surfaces.[100] In this approach a bifunctional ligand was used as the base layer, bearing a cyclic disulfide group for attachment to the gold surface and a bishydroxamate group capable of ion binding (Zr^{4+} or Ce^{4+}). The chelated metal ion was then used for coordination of a second ligand possessing four hydroxamate groups. Successive addition of metal ions and tetrahydroxamate led to the formation of a well-defined multilayer. The biospecific interactions between the lectin protein Concanavalin A (Con A) and a mannose-labeled enzyme were exploited also in LBL assembly, and it showed that the Con A–sugar complexation was a useful tool for constructing multilayer thin films of proteins.[103]

What is unique for LBL assembly in comparison with other film deposition techniques is the broad range of materials that is available for incorporation in a multilayer thin film, and the

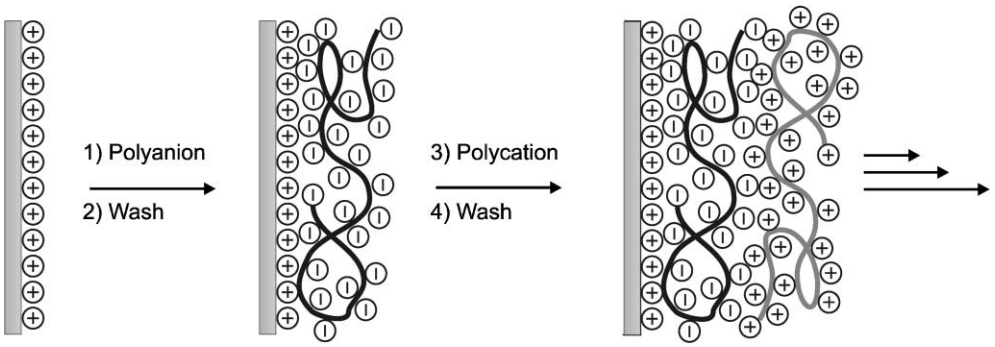

Fig. 6 Concept of layer-by-layer assembly, depicting film deposition of two complementary polyelectrolyte species.

versatility of the number of interactions available for such assemblies. Some of these materials include polymers,[96] inorganic nanoparticles (paragraph 3.2), clay,[105] organic components,[106] carbon nanotubes,[107] dendrimers,[108] and biological macromolecules such as proteins[109] and DNA.[110] LBL assembly is therefore emerging as an inexpensive and versatile technique to create electro-optical, conducting sensors and perm-selective, luminescent films.[96]

In general, multilayer films show a linear growth of mass and thickness, although a second class of films have been reported in which mass and thickness grow exponentially with the number of deposition steps.[111]

3.2 Nanoparticle multilayer films

Of special interest is the multilayer assembly of inorganic NPs. The incorporation of inorganic NPs or their precursors through direct adsorption into the multilayer thin films has been demonstrated to yield closely packed layers of NPs homogeneously distributed throughout the multilayer film[95,96]. NP multilayer films are of great importance for sensing and electronic applications.

One of the most simple and versatile methods for the construction of ultrathin organized NP multilayers is the electrostatic LBL assembly of NPs and polyelectrolytes.[60] The driving forces for the assembly are the electrostatic interactions between the charged groups in the outer layer of the film and the charged groups at the particle surface, enabling the creation of 2D structures in a stepwise fashion. One of the advantages of using polymers for NP assembly is the possibility of fabricating hybrid materials that incorporate not only metal and semiconductor NPs, but also different polymers with different properties, such as conducting[112,113] or redox active polymers.[114] Moreover, electrostatic NP arrays can be constructed from any charged NP and any oppositely charged crosslinker with the same protocol as in the polymer–colloid multilayers. The crosslinker can be any type of molecule, the only prerequisite is the presence of multiple charges, so that it can simultaneously interact with several colloidal layers. For example, thin films of silver NPs were incorporated into generation 1 and 5 PPI dendrimers, giving different optical properties depending on the generation and concentration of dendrimer used.[115] Moreover, dendrimers with higher generations can also be used to encapsulate NPs, therefore metal–dendrimer nanocomposites can be prepared using dendrimers with various terminal groups able to interact with each other. Esumi and co-workers studied the LBL formation using a positively charged gold–dendrimer nanocomposite and a negatively charged silver–dendrimer nanocomposite. The dendrimer carrier used for the assembly was a generation 5 polyamidoamine (PAMAM) dendrimer (Fig. 7).[116]

Multilayers of particles can be also produced by alternate immersion into a solution of functional crosslinker and NP solutions, which produce random arrays of NPs of controllable thickness. For example, this has been accomplished by the use of bisthiol crosslinkers for gold.[117] If the gold NP monolayer is exposed to a solution of a bisthiol, then the crosslinker assembles on the gold surface, which leaves thiol

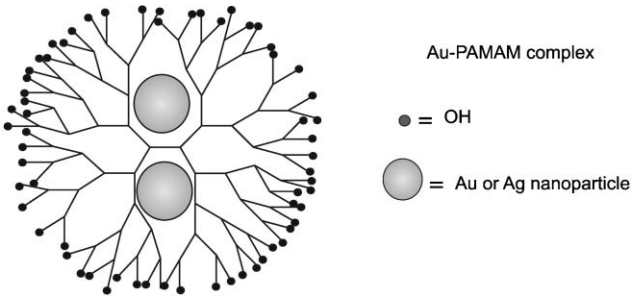

Fig. 7 Schematic picture of a PAMAM dendrimer encapsulating NPs.[116]

moieties at the nanostructure–solution interface. The assembly of a second colloidal layer is thereby possible and the construction can continue in the same way. The versatility of the method, depending on the type of functional groups used as crosslinker, allowed the construction of multilayers of different nanoparticle composition.[118]

Coordination chemistry offers stable bonding and metal–ligand specificity, so that ligand-bearing NPs can be assembled at surfaces using the appropriate metals ions. This approach is particularly compatible with multicomponent construction systems since binding of the metal ions activates the surface toward NP-ligand binding, and *vice versa*. The use of different building blocks containing similar ligand functionalities provides a general method to assemble NP arrays and NP multilayer films on surfaces. The first example of coordinated NP films was described by Murray and co-workers. The procedure consists of the repetitive adsorption of carboxylate-modified gold NPs and divalent metal ions (Cu^{2+}, Zn^{2+}, Pb^{2+}) on two different types of anchoring surfaces, gold and silicon oxide with carboxylate-terminated SAMs.[119–121] Repeated dipping cycles resulted in the formation of network NP films. This NP network exhibited electrical conductivities that could be varied by both the number of methylene segments in the ligands and the medium.[122] However, in this type of coordination-based NP networks, the interparticle distance was shown to be lower than expected for a coordinative carboxylate-metal ion binding (and also the absorbance changes were much larger that those expected for a LBL film growth). Chen and co-workers obtained similar results with pyridine-functionalized gold NPs and Cu^{2+} ions, studied by quartz crystal microbalance (QCM) measurements.[123] These observations suggested that the excess surface-coordinated Cu^{2+} could migrate out toward the NP solution resulting in a poorly controlled NP network growth. In an attempt to achieve controlled growth of NP films, Rubinstein and co-workers reported the construction of monolayer and multilayer NP architectures on surfaces by coordination chemistry with Zr^{4+} ions (Fig. 8).[124]

We have developed a supramolecular procedure for the stepwise construction of multilayer thin films.[125] This method is based on multivalent supramolecular interactions between guest-functionalized dendrimers and host-modified gold NPs, yielding supramolecular layer-by-layer assembly (Fig. 9). The deposition process was monitored by surface plasmon resonance (SPR). Further characterization of the multilayer

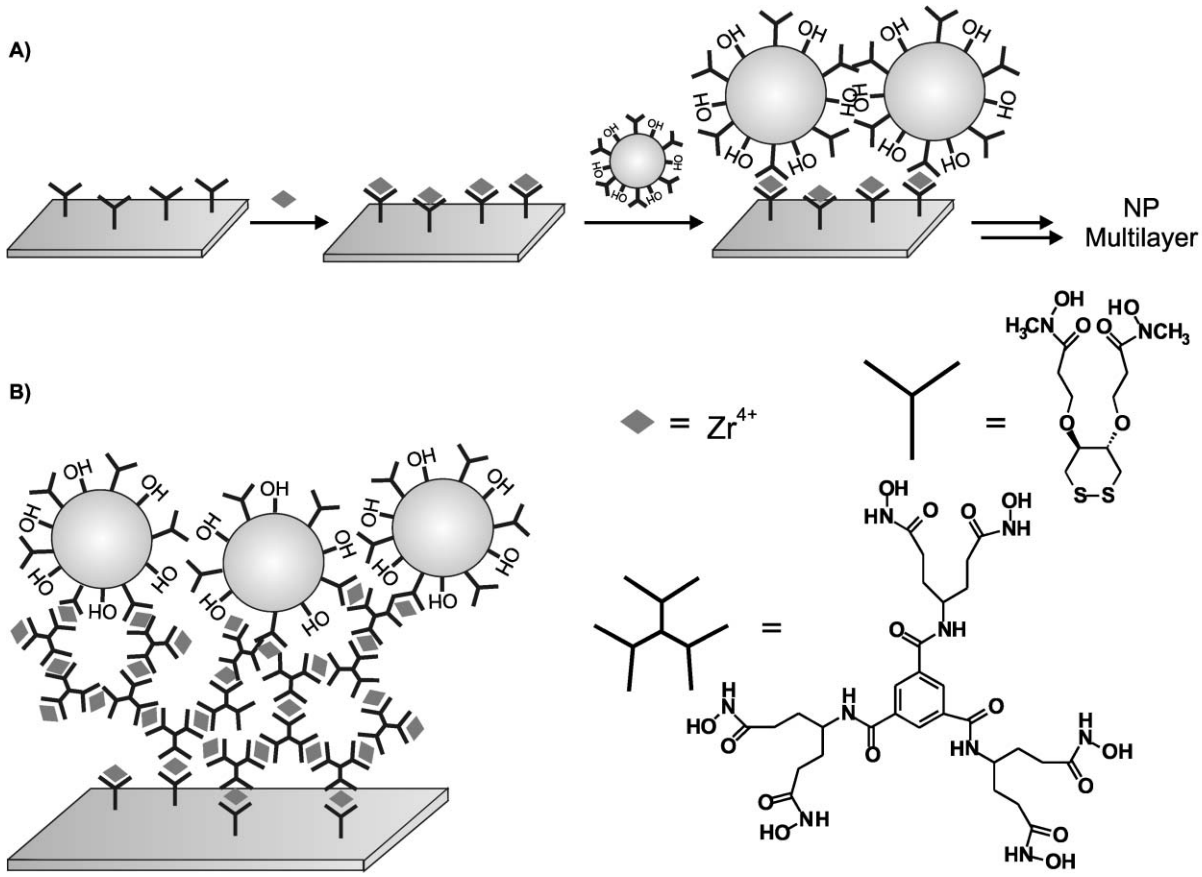

Fig. 8 Schematic representation of: (A) stepwise assembly of bishydroxamate gold NPs onto a bishydroxamate disulfide SAM on a gold surface through the coordination of Zr^{4+} ions. (B) Spacing of a NP monolayer from the gold surface using a similar metal-coordination approach.

films performed by UV–vis spectroscopy, showed a linear increase of absorbance with the number of bilayers. The growth of the gold NP plasmon absoption band corresponded to approximately a dense monolayer of gold NPs per bilayer. Ellipsometry and AFM scratching experiments confimed a linear growth and a thickness increase of approximately 2 nm per bilayer.

The incorporation of semiconductor quantum dots (QDs) into multilayer thin films has been of interest for the use in fluorescence and luminescent detections methods. For example, Kotov and co-workers demonstrated that LBL methods can be used to build graded semiconductor composite films of highly luminescent CdTe.[126] Four different CdTe NPs were used; these particles displayed green, yellow, orange, and red luminescence spectra due to their differences in particle size and were alternately dispersed with a strong polycation and deposited on glass and plastic supports. After adsorption of ten layers, the resulting film exhibited a clear gradient in nanoparticle size and therefore density across the thickness of the film, thus yielding a ''rainbow'' of colors. The purpose of the study was on the construction of multilayer nanoparticle films to exhibit energy transfer effects across the gradient films, which could be useful for photovoltaic applications.

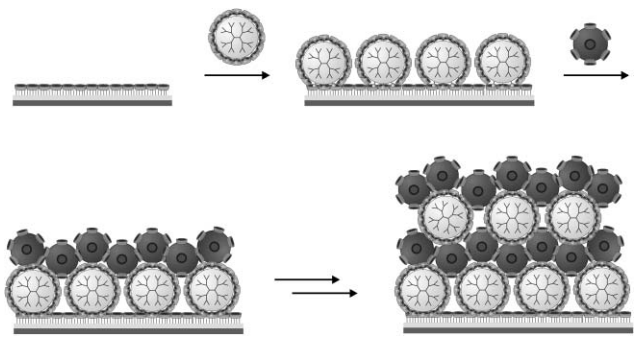

Fig. 9 Layer-by-layer assembly scheme for the alternating adsorption of adamantyl-terminated PPI dendrimers and CD gold NPs onto CD SAMs.[125]

3.3 Multilayer templating on particle surfaces

Most of the approaches discussed in the previous sections address the formation of structures built up from 2D surfaces. However, uniform multilayers can also be formed on a number of 3D objects. The most common system types of LBL assembly on colloidal particles is the electrostatic deposition of polyelectrolytes (Fig. 10). This capability was first demonstrated by Donath, Caruso, Möhwald and co-workers.[127,128] The approach is based on the consecutive adsorption of polyelectrolytes on the surface of negatively charged polystyrene and melamine formaldehyde latex particles. Besides polyelectrolytes, a number of other synthetic components ranging from inorganic nanoparticles,[129–133]

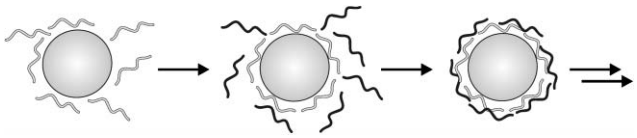

Fig. 10 Schematic illustration of the polyelectrolyte deposition process in colloid-templated electrostatic layer-by-layer assembly.

DNA,[110] lipid bilayers,[134] and proteins[135] have been used to fabricate new LBL colloidal type nanostructures with controllable thickness and composition at the interfacial region. Thus, this methodology permits remarkable control over the coating uniformity and thickness, and the high level of flexibility allows the design, structure and properties of the resulting particles to be varied tremendously. This area of the field has been expanding rapidly and it has been well covered by several reviews.[129,136]

Individual layers of inorganic nanoparticles can be incorporated into the multilayers, including silica, gold, silver, and iron oxide.[129–133] The assembly of a dense layer of nanoparticles on colloidal particles includes the use of electrolyte or other synthetic material shielding, to prevent repulsive interactions and to enable the dense packing of nanoparticles enabling the formation of shells on the colloid surface. Depending on the nature of the nanoparticle, the LBL colloidal nanocomposite can lead to materials with magnetic properties,[133] or different optical response depending on the morphology of the building blocks;[131] besides they can also be used as sites for further electroless deposition.[130]

Additionally, it was found that decomposition or dissolution of the templating core could yield hollow microcapsule shells consisting of the free LBL assembled films in the form of the original NP shape.[127,129] This process required the dissolution in organic solvents or calcination of the polystyrene particles or the dissolution of melamine formaldehyde particles in acidic solution. The two different processes can lead to different morphologies of hollow spheres (Fig. 11).[129] The nanoscale morphology was reported by Decher *et al.* who used gold NPs to create hollow nanospheres. Dissolution of the gold core was achieved under vigorous stirring of the particle suspension in a solution containing an excess of KCN.[137] The thickness of the hollow sphere walls can be controlled by the number of layers deposited, size, shape and composition of the spheres, which can be easily determined by the templating colloid employed and the incorporation of different materials. Because of the versatility of the system and the generally flexible membrane, these hollow structures have interesting potential applications as micro- and nanocarriers for molecules and nanoparticles, as well as biological species for the controlled release and targeting of drugs, catalytic nanoreactors, and photonic materials.[136,138,139]

Similarly to the LBL assemblies on flat surfaces, the incorporation of quantum dots (QDs) in the interior of these templated colloids has also been achieved. Li and co-workers described an example in which magnetic luminescent nanocomposites composed of Fe_3O_4 and CdTe were prepared. Fe_3O_4 nanoparticles were used as a template for the deposition of three polyelectrolyte–CdTe QD multilayers. It was found that the photoluminescence properties of the magnetic luminescent nanocomposites could be tuned by controlling the distance of the polyelectrolyte interlayer between the magnetic nanoparticles and QDs and the CdTe QD loading of the nanocomposites.[140] Additionally, the authors used magnetic fields for the separation and redispersion process of the nanocomposites.

Spherical particles are not the only ones which can act as templates. Multilayers on coated cells have been prepared, on which a perfect, ultrathin membrane was formed around an individual cell.[141] Other geometries such as nanotubes from human serum albumin (HSA) were prepared by the alternate adsorption of the respective positively and negatively charged species on the inner walls of an alumina template membrane. After subsequent removal of the template, free-standing HSA nanotubes were obtained.[142] Highly porous materials such as porous calcium carbonate particles can be used as template materials as well. The use of these types of templates results in

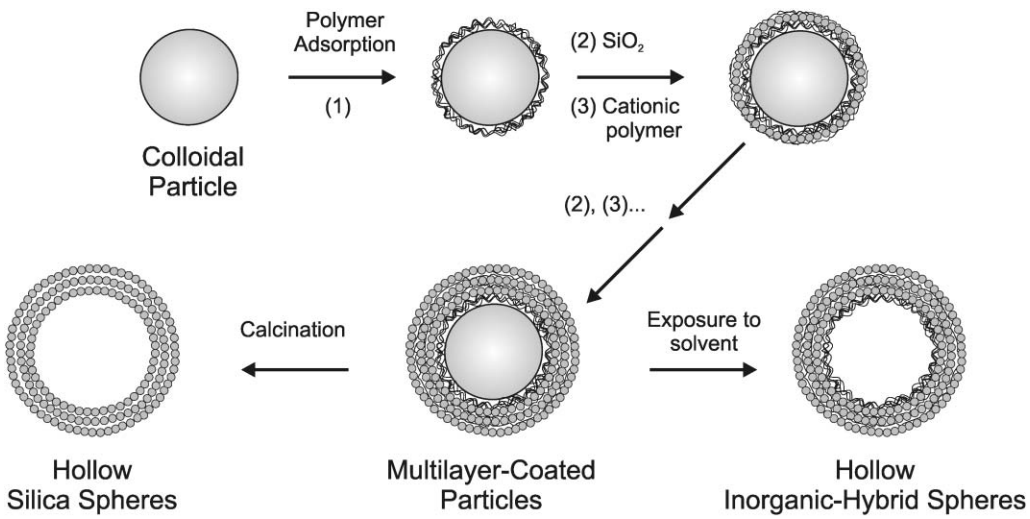

Fig. 11 Illustration of procedures for preparing hollow inorganic silica and inorganic-hybrid spheres through the colloid-templated electrostatic LBL assembly of silica NP polymer multilayers, followed by the removal of the templating core and, optionally, the polymer.[129]

the formation of thin films on the exterior surfaces as well as on the interior pores of these particles.[143]

3.4 Methods to pattern multilayer thin films

LBL allows the tuning of thin film compositions at the nanometre scale and, when combined with inexpensive patterning routes, provides a powerful tool for patterning nanometre to micrometre-scale assemblies.[96]

The first micropatterning approach was reported by Hammond and co-workers in which they utilized the concept of selective deposition on chemically patterned surfaces.[144–147] The driving force of the approach is the use of secondary or nonspecific interactions, in combination with steric repulsion and electrostatic interactions, to chemically direct the deposition of polyelectrolytes on chemically patterned substrates. Thus, one surface region supports the build-up of the LBL assembly, whereas the alternate region acts as a resist to deposition. The approach described by Hammond's group employed microcontact printing techniques to create SAMs of micrometre-scale features on surfaces of the desired functional groups. Carboxylic acid-functionalized SAMs, alternating with an oligo(ethylene glycol) (EG) SAMs were immersed in solutions of the respective polyelectrolytes to build up patterned multilayer films. Oligomers of EG are known to act as hydrated brushes in aqueous solution, thus preventing the adsorption of polyions due to repulsive forces and enthalpic penalties for disruption of the hydrogen bonds EG forms with water. However, the region of preferred deposition on a chemically patterned surface can be influenced by hydrogen-bonding and hydrophobic interactions, as well as electrostatic interactions, between the charged polymer and the surface. For example, certain polyamines consistently adsorbed to the EG region of the surface due to non-electrostatic interactions, resulting in some cases in preferential build-up of multilayer films on the EG region. This behavior was observed in the adsorption of weak polyelectrolytes for which the degree of ionization is dependent on pH, and secondary interactions may prevail over given pH range.[146] Similar studies by the same group showed that at very high salt concentrations, polyelectrolyte deposition can be reversed creating a negative of the original positive structure.[145] So far, this method has only been applied to micrometre features, but the ability of this methodology to gain smaller feature sizes at a nanometre lengthscale was recently demonstrated by Jonas an co-workers.[148] Electron beam lithography followed by gas-phase silanation was utilized to create chemical patterns to direct LBL assembly with features down to 150 nm dots. The selective deposition is easily achieved when systems of different compositions are being assembled on a surface. However, when thin film compositions are similar in nature, it is challenging to create patterned surfaces onto which such systems will adsorb selectively.

The selective deposition described above demonstrates the advantage of soft-lithographic methods; however, multilayer thin films can also be patterned using photopatterning techniques. The most common approach uses a photo-cross-linkable polyion in the multilayer thin film. This was demonstrated through the use of diazoresins to create multilayers in

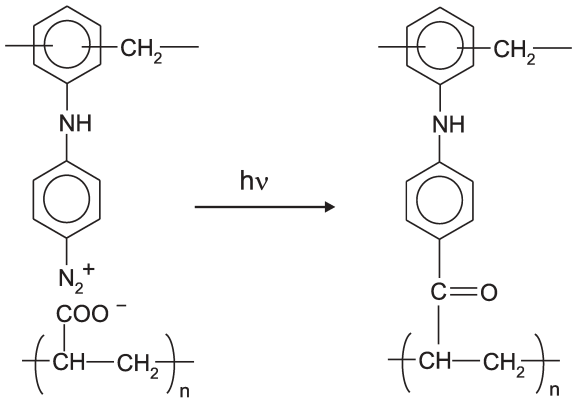

Fig. 12 Schematic representation of the reaction between diazo-resins and poly(acrylic acid) in a multilayer assembly upon UV irradiation.

which photocrosslinking stabilizes specific regions of the film.[149–153] After the LBL assembly, the substrate is exposed to UV irradiation through a photomask, causing crosslinking in the polyelectrolyte regions exposed to UV light. The films were then exposed to a surfactant solution containing sodium dodecyl sulfate, which caused the dissolution of the unexposed film areas. Despite the versatility of the procedure, it requires the introduction of a photo-crosslinkable monomer into the LBL assembly (Fig. 12).

A different technique was introduced by Lvov and co-workers, who used a metal mask in combination with a lift-off approach to pattern LBL assemblies of more than one type of NPs.[154,155] A silicon substrate was coated with a multilayer film of polystyrene particles on top of which aluminum and photoresist layers were deposited subsequently. After UV irradiation through a photomask and exposure to an aluminum etchant, a layer of different silica particles was deposited on top. After lift-off of the photoresist and aluminum, a pattern with two types of particles was obtained (Fig. 13).

Moving towards the construction of more complex, 3D structures, Hammond's group developed a technique consisting of LBL assembly on a PDMS relief stamp which allowed subsequent transfer of the LBL structures onto a substrate in the contact areas.[156] This approach resembles nanotransfer printing (nTP) developed by Rogers *et al.*[157] We have developed various patterning strategies to create 3D structures of supramolecular LBL assemblies on molecular printboards.[125,158] nTP and NIL were used to obtain faithfully

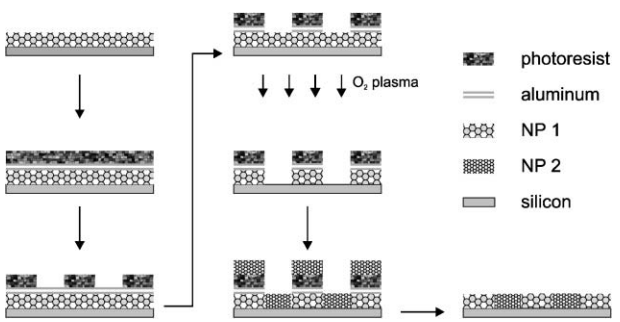

Fig. 13 Schematic representation of the combination of a metal mask with a lift-off approach to pattern multilayers of two types of NPs.[155]

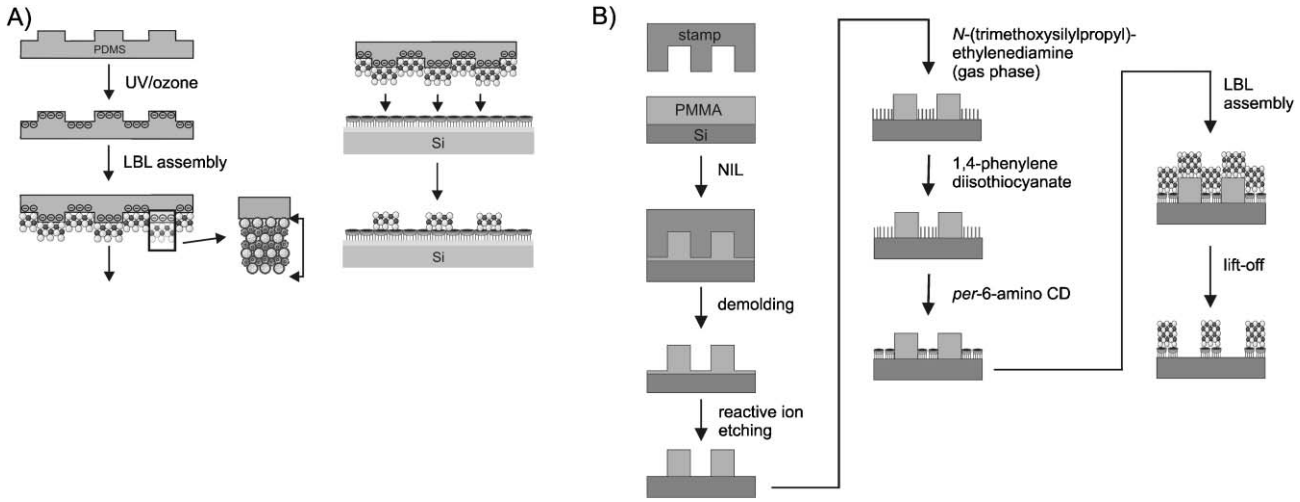

Fig. 14 (A) Preparation of supramolecular patterned LBL assemblies by nTP. (B) Preparation of NIL-patterned LBL assemblies using NIL, CD monolayer formation, and LBL assembly and lift-off.[158,159]

patterned supramolecular LBL assemblies on the CD SAMs. nTP was achieved by LBL assembly on a PDMS stamp followed by transfer onto a full CD SAM (Fig. 14A). NIL-prepared PMMA patterns provided patterned CD SAMs and functioned as a physical mask for LBL assembly (Fig. 14B). These LBL assemblies showed good stability against rinsing, even with a monovalent competitive host in solution, and against acetone/ultrasound treatment. High-resolution 3D nanostructures were obtained using high-resolution masters.[159]

So far, the above methodologies described the patterning of multilayers onto substrates. However, it would be desirable to pattern a single layer of a chemical functionality on top of an existing layer. Therefore, Hammond and co-workers developed the so-called polymer-on-polymer stamping (POPS) technique (Fig. 15).[160] In this approach chemical patterns were obtained by the direct stamping of functional polymers onto a surface containing complementary functional groups. The resulting pattern was then used as a template for the deposition of materials on the surface. The versatility of this method allows the functionalization of surfaces with a number of different functional groups. POPS has been used as a template for the attachment of inorganic NPs,[63,161–163] cells,[164,165] microcapsules,[166] and to generate electroless plated metal patterns.[167]

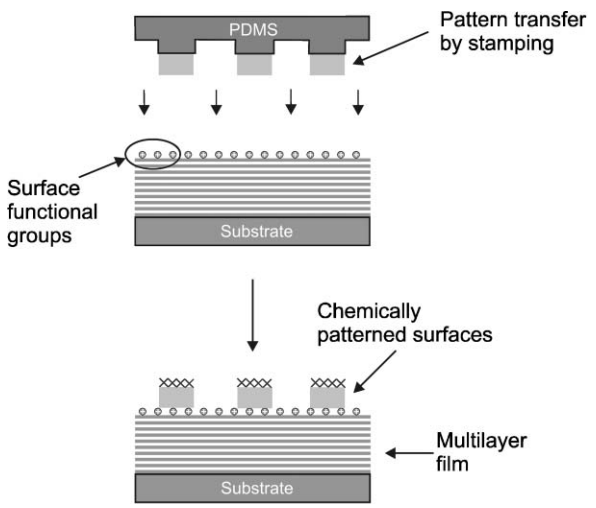

Fig. 15 Schematic illustration of the transfer of a functional polymer to a surface with complementary functionality using polymer-on-polymer stamping (POPS).[160]

4. Templated nanoparticle assembly for 3D nanoarchitectures

During the last decade substantial research has been focused on metal (Au, Ag, Pt, Cu) and semiconductor (PbS, Ag_2S, CdS, CdSe, TiO_2) NPs, partially as a consequence of the development of methods to control particle size and also to stabilize the particles in solution.[4,168] One possible approach is to passivate the surface of the NPs with an organic monolayer that protects them from aggregation and provides functional and specific chemical properties.[169,170] The versatility of physical and chemical properties of metal and semiconductor NPs makes them promising as miniature devices, with potential applications ranging from optoelectronics[171] and sensing[60] to catalysis[172] and biology.[82,173] They also provide building blocks for more complex systems. Organization of functional NPs into spatially well-defined arrays provides a powerful tool for the creation of materials structured at the nanometre level, and to extend the prefered properties of these materials to the macroscopic level.

This section is focused on the different methodologies to create and control NP assembly into well-defined nanoarchitectures based on non-covalent interactions. One-dimensional (1D) assemblies are described in other reviews.[174] First, NP assembly that is based on supramolecular recognition and the different non-covalent interactions that have been used for NP assembly will be described. In the last section NP assemblies induced by specific biological interactions will be described.

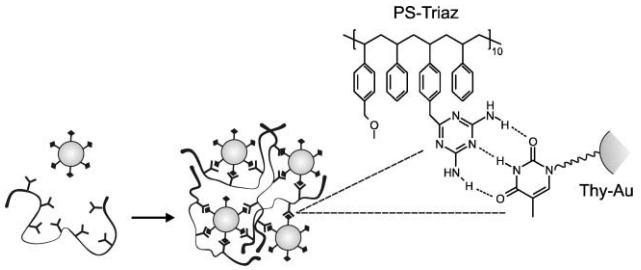

Fig. 16 NP–polymer assembly through a three-point hydrogen bonding between thymine-functionalized gold NPs and triazine functionalities attached to a polystyrene backbone.[176]

4.1 Nanoparticle assembly by molecular recognition

The controlled assembly of NPs in solution based on non-covalent bonding is a general strategy that leads to organized NP materials. Various approaches have been reported using hydrogen-bonding, host–guest, metal coordination, electrostatic, charge-transfer, and π–π interactions. This section is dedicated to recent examples of the use of these interactions to assemble NPs into well-ordered 3D nanostructures.

4.1.1 Hydrogen-bonding-directed nanoparticle assembly. Molecular recognition through multiple hydrogen-bonding interactions has been widely used to create complex 3D structures in solution. The use of multiple hydrogen-bonding interactions allows assembly at near-equilibrium conditions, which facilitates control over the thermodynamic parameters of the assembly.

Fitzmaurice and co-workers have described an example of a three-point hydrogen-bonding interaction for NP assembly. In this approach, gold NPs were prepared by a chemisorbed mixture of dodecanethiol and a uracil receptor. Addition of a molecule incorporating a diaminopyridine substrate resulted in the formation of a 1 : 1 complex associated by a triple array of complementary hydrogen bonds.[175]

Rotello and co-workers have developed a polymer-mediated ''bricks and mortar'' strategy for NP assembly. They have utilized a polymer scaffold and NPs that are functionalized with complementary recognition units[176] and have reported their use for different applications such as chemical sensing and catalysis.[177] Diaminotriazine–thymine three-point hydrogen bonding interactions were employed to obtain complementarity between thymine-functionalized gold NPs (Thy-Au) and diaminotrazine-functionalized polystyrene (poly-Triaz).[178] Addition of poly-Triaz to a concentrated solution of Thy-Au in nonpolar solvents resulted in the formation of spherical aggregates (Fig. 16). In contrast, no precipitation was observed when the control MeThy-Au NPs were used, demonstrating the role of specific three-point hydrogen bonding for the formation of poly-Triaz–Thy-Au aggregates. The temperature at which the assembly process was performed had a tremendous effect on the diameter and the morphology of these aggregates. At room temperature TEM images showed the formation of large spherical clusters comprising 3000–7000 individual gold NPs. Performing the assembly at −20 °C yielded to 5–10 times larger clusters.[176]

In an effort to provide a component-based mechanism of control over aggregate size, Rotello and co-workers replaced the functionalized polystyrene random copolymer with diblock copolymers, where one block that was analogous to the previous poly-Triaz was covalently linked to an ''inert'' polystyrene block.[179] Three symmetric diblock copolymers of different lengths were used as the 'mortar'. The NP assembly resulted in spherical aggregates with diameters that directly correlated with the length of the functionalized block copolymer. Combined measurements of average core size (from TEM) and overall aggregate size (from DLS) indicated that the polystyrene chains decorating the exterior made up for less than half of the overall aggregate radius, suggesting that the polymer chains within the core are somewhat extended relative to the polystyrene corona.

Rotello and co-workers extended the repertoire of aggregate compositions by preparing a novel type of large-scale assemblies composed of diaminopyridine-functionalized poly-oligosilsesquioxane (POSS) and thymine-functionalized NPs assembled through three-point hydrogen bonding (Fig. 17).[180] The same group reported the use of polymer-mediated self-assembly to modulate the physical and functional properties of

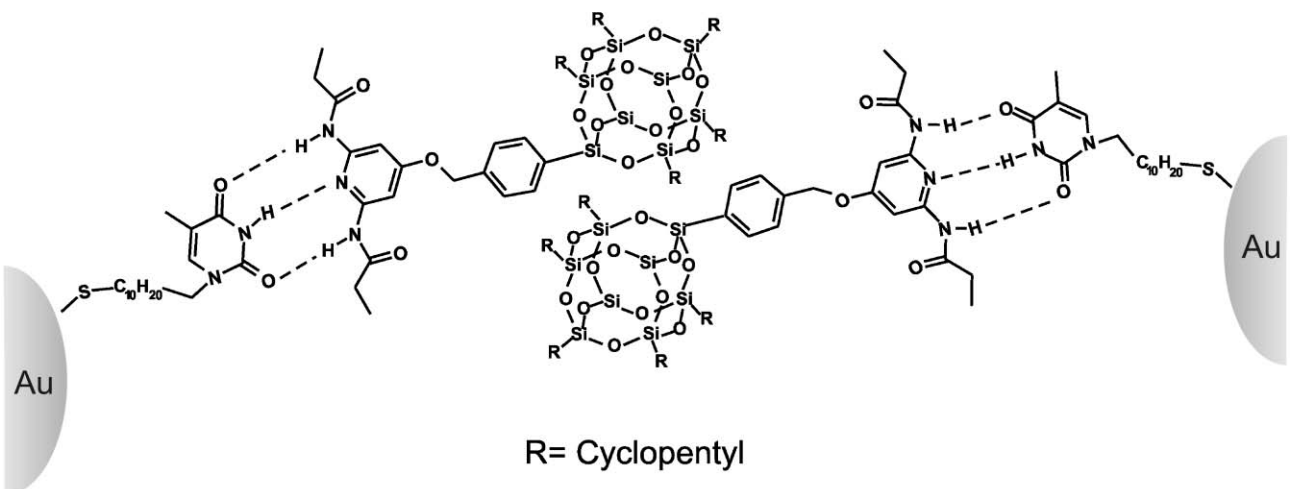

Fig. 17 Thymine-functionalized NPs and diaminopyridine-functionalized POSS showing three-point hydrogen bonding.[180]

γ-Fe_2O_3 NPs aggregates while retaining the magnetic properties in the assembly.[181] Additionally, gold NPs capped with a thiolate shell and alkanethiols terminated with carboxylic acid groups were employed to construct network architectures *via* hydrogen-bonding linkages at the carboxylic acid shell.[182]

Not only have different methodologies and different compositions of hydrogen-bonded NPs assemblies been studied, the structure and dynamics[183] as well the kinetics[184] of the assembly have also been investigated carefully. Rotello *et al.* found that both structure and dynamics of the assembly can be controlled by the incorporation of internal, intramonolayer hydrogen-bonding elements (amide-functionalized NPs). Thus, when the distance between the amide functionality and the core increases, the disorder of the monolayer increases, making the intramonolayer interactions more entropically disfavored. Additionally, NPs with an amide functionality near the exterior of the monolayer bind intermolecularly to other NPs creating large amorphous self-assembled NP networks.[183] The aggregation kinetics of the assembly was also studied by Fitzmaurice *et al.* who found that the kinetics of NP aggregation, and as a consequence the structure of the resulting NP aggregates, depends on the number of receptor sites at the surface of the NPs.[184]

4.1.2 Nanoparticle assembly by inclusion interaction. NP assembly has been performed using host–guest inclusion as the driving force for the assembly, resulting in the formation of 3D nanostructures. Cyclodextrins can be incorporated into the monolayer of NPs to provide a motif for molecular recognition. Kaifer and co-workers developed a modified CD system that was immobilized on the surface of platinum,[185] palladium,[186,187] silver,[188] and gold.[189] The same group studied the formation of supramolecular aggregates between β-cyclodextrin functionalized NPs and a divalent bis(ferrocene).[189] The addition of the bis(ferrocene) to a solution of β-cyclodextrin NPs resulted in the formation of large network aggregates, which eventually precipitated. Addition of a competitor in solution, either ferrocene methanol or free β-cyclodextrin, did not lead to any precipitation or flocculation of the NPs. Additionally, decrease of concentration and increase of temperature slowed down the kinetics of precipitation. The same behavior was observed for γ-cyclodextrin-modified gold NPs in combination with C_{60} fullerene molecules.[190]

We have studied the formation of large network aggregates composed of gold NPs bearing surface-immobilized β-CD hosts, whose assembly is driven by adamantyl-terminated guest molecules by employing strong, specific, and multivalent host–guest interations.[191] This process, employing guest systems that can give intra- and intermolecular binding, could be controlled by the number of interactions available for the assembly, the geometry of the molecules, and by adding a competitor in solution to prevent aggregation.

Another approach to incorporate inclusion-based host–guest recognition is through the use of pseudorotaxane assemblies. To integrate this motif into NP systems, the groups of Fitzmaurice and Stoddart have synthesized gold NPs featuring dibenzo[24]crown-8 ether moieties on the surface.[192] Through NMR experiments it was shown that these NPs formed pseudorotaxanes on the surface by binding dibenzylammonium cations. The same groups studied the possibility of forming NP assemblies based on the same pseudorotaxane formation.[193] In this study silver NPs were stabilized by chemisorption of an alkanethiol–dibenzo-24-crown-8 adsorbate mixture. Addition of a stochiometric amount of a bis-dibenzylammonium dication initiated the aggregation of the dibenzo-24-crown-8 silver NPs, leading to the formation of larger aggregates through [3]pseudorotaxane complexes (Fig. 18). Like Kaifer *et al.* reported for the cyclodextrin-modified NPs,[189,190] control over the NP assembly was demonstrated by the addition of an excess of the receptor or of the substrate which inhibited aggregation.

Pseudorotaxane recognition was applied to binary NP structures assembled in solution from silver NPs surrounding silica NPs.[194] The assembly consisted of dibenzo[24]crown-8-modified silver NPs and dibenzylammonium-modified silica NPs, where the cation was generated in situ at the surface of the silica NPs by photolysis and subsequent protonation. The recognition of the silica NPs by silver NPs led to the pseudorotaxane formation at the surface of the NPs and subsequent aggregation. Thermal annealing led to an irreversible coating of silver around the silica beads.

4.1.3 Metal ligand-directed nanoparticle assembly. Metal–ligand systems provide a means of expanding the structural diversity of self-assembly processes.[195] To explore the application of this methodology to nanocomposite fabrication, Rotello's group has synthesized NPs bearing terpyridine

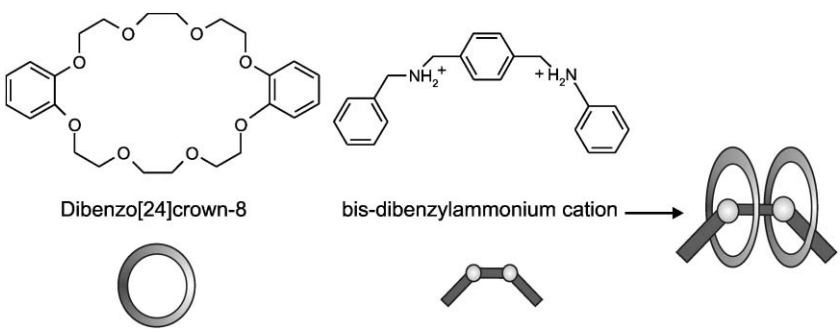

Fig. 18 [3]Pseudorotaxane formation induced-NP assembly is due to the recognition and selective binding of dibenzo[24]crown-8 and bis-dibenzylammonium cation.[193]

(terpy) ligands and studied their self-assembly using a variety of transition metals.[52] Metal-induced aggregation of NPs was obtained with Fe, Ag, Zn, and Cu ions. Aggregates formed by the addition of the weaker tetracoordinate complexes (Ag, Cu) appeared to be more dense as a result of a thermodynamically controlled assembly process, which allows for reorganization and optimization of coordination interactions within the assembly. The stronger hexacoordinated terpy complexes formed very rapidly and resulted in aggregates filled with many voids and cavities. The overall strength of the assemblies could be controlled through the choice of bridging metal ions. In a similar experiment, Murray and co-workers controlled the formation of aggregates of thiopronin-modified NPs by the addition of Cu^{2+}. The amount of Cu^{2+} required to induce NP assembly was strongly dependent on pH and increased at lower pH, where the thiopronin acid groups were protonated making them no longer available to chelate the Cu^{2+} ions.[120]

One characteristic of gold NPs is the relatively high extinction coefficient that makes them very attractive as colorimetric reporters for particular metal ions. Hupp and co-workers prepared 11-mercaptoundecanoic acid-capped gold NPs that aggregated in solution in the presence of divalent metal ions like Pb, Cd, and Hg by an ion-templated chelation process.[196] The aggregation process was monitored through changes in the adsorption spectrum of the particles. The process could be reversed by the addition of a strong metal ion chelator such as EDTA.

One of the limitations of developing organic chromophores for practical Li^+ detection is their lack of solubility in aqueous media. To overcome that problem, Murphy and co-workers designed a detection system based on NP aggregation.[197] Gold NPs were functionalized with 1,10-phenanthroline derivatives, which are particularly selective for Li^+. Addition of Li^+ to the NP solution resulted in a color change of the solution followed by precipitation. The sensitivity for Li^+ was tested as a function of NP size, showing that smaller NPs have lower detection limits.

In contrast to the previous studies, Chen and co-workers developed a more specific method for metal-ion sensing with gold colloids.[198] They attached crown ether receptors onto a gold NP in order to detect the presence of K^+ over Li^+, Cs^+, NH_4^+, Ca^{2+}, and Na^+. Upon addition of Na^+ to the modified 15-crown-5 gold NPs, stable complexes were obtained. However, the addition of K^+ to the Na^+-NP complexes resulted in the formation of aggregates composed of a "sandwich complex" of 2 : 1 15-crown-5 and K^+.

4.1.4 Nanoparticle assembly by electrostatic interactions. Rotello and co-workers described the assembly of two different types of NPs through electrostatic interactions.[199] Their strategy involved the functionalization of one type of colloidal building block (SiO_2 NPs) with a primary amine, and a counterpart (gold NPs) with a carboxylic acid derivative. By combining the two systems, acid–base chemistry followed by immediate ion-pairing resulted in the spontaneous formation of electrostatically bound mixed-colloid constructs. The shape and size of these ensembles was controlled by variation of particle size of the two components and their stoichiometry. A more elegant multi-component electrostatic self-assembly protocol was proposed by the same group a making use of the "bricks-and-mortar" system with a polymer serving as a matrix for the controlled assembly of nanoparticles.[177] Carboxylic acid-terminated gold and silica NPs were employed together with an amine-functionalized polystyrene random copolymer. In this three-component system, electrostatic interactions between the basic polymer and the acid-functionalized NPs resulted in the formation of diverse structures. Control over the assembly process was provided through the order of the component addition. For example, when the polymer was added to a mixture of the two NPs, well-integrated nanocomposites were obtained. However, premixing of the silica NPs with the polymer followed by addition of the gold NPs led to segregated clusters, where the gold NPs were exposed at the surface of the supporting silica aggregates.[200]

Weller and co-workers studied the self-organization of positively and negatively charged CdS NPs, and negatively charged gold NPs in order to obtain 3D ordered NP systems.[201] Mixing of the two different nanoparticle solutions led to different superlattices depending on the ratio of the positive to negative charges. The particles were stable in solution if one of the components was in excess, while precipitation occurred if the ratio was close to one. NP aggregates could be redissolved or precipitated by changing the ionic strength of the solution. Using similar methodologies, hybrid inorganic–organic composite materials composed of gold colloids and polyhedral oligomeric silsesquioxane (POSS) were prepared by the groups of Rotello[202] and Chujo.[203] These assemblies feature uniform and rigid interparticle spacings consistent with the POSS diameter.

Another approach for NP assembly has focused on the use of amino acids (which bind to gold NPs with their amino groups) as binding agents. Their control of aggregation depends on the reactivity of the α-amine, which is found to be pH-dependent. Linking *via* the α-amine is activated at low pH but suppressed at intermediate and high pH due to electrostatic repulsive forces between the gold surface and the charged carboxylate groups or even the (formally neutral) polar carbonyl groups in amides. However, dibasic amino acids can still be used to crosslink gold colloids at high pH.[204] Two different aminoacids have been used for such an approach, cysteine (Cys)[205] and lysine (Lys).[206,207] In the case of Cys, the two functional groups (SH and NH_2) are able to bind gold with different abilities, the SH group binds readily, whereas the α-amino group displays pH-dependent behavior. In the case of Lys two chemically distinct amino groups determined the ability to bind gold and organize the NPs into supramolecular aggregates. By adjusting the pH, starting concentrations and surface charge (by way of the Au : aminoacid ratio), the aggregation process could be manipulated to produce a structure of desired size and shape. In the case of Cys, a pH range of 7–10 and Au : Cys molar ratios of 1 : 0.5–1 : 2 resulted in the formation of spherical aggregates.[205] For Lys, at a pH range between 8–10 and a molar ratio of 0.5, linear gold aggregates were obtained.[206] Additionally, NP assemblies could be adjusted from spherical-like to chain-like by mixing Cys and Lys in various ratios.

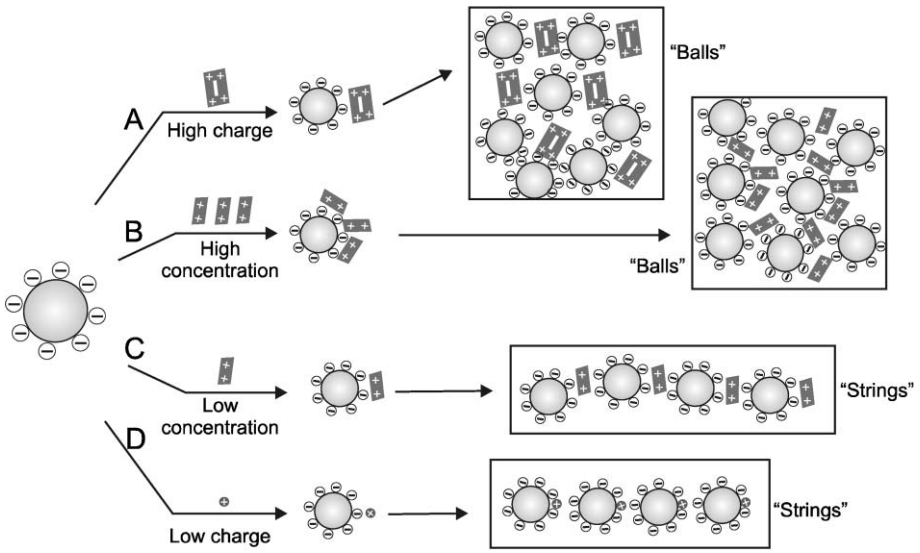

Fig. 19 Possible mechanisms for the formation of ''string-like'' and ''ball-like'' aggregates of gold NPs based on crosslinker charge and concentration.[209]

Several factors can influence the stability and morphology of NP aggregates. The pH and the ionic strength have a huge influence on electrostatically induced NP assembly due to the presence of ionizable groups on the particle surface.[208] However, also charge density and concentration of crosslinkers affect the formation of such assemblies (Fig. 19).[209] Crosslinkers with a high charge or high concentration can neutralize the particle's zeta potential, facilitating the formation of tightly bound aggregates. On the other hand, crosslinkers with a low concentration or charge do not allow the full neutralization of the zeta potential, so they are ineffective at bridging the NPs together into stringlike aggregates. The elimination of excess free ions results in an appropriate balance of repulsion and attraction among colloids which leads to their self-assembly into 3D cluster-type aggregates.[210]

As mentioned before, the physical properties of NPs are affected by neighboring particles in a strongly distance-dependent interaction.[211] Controlling interparticle distance has been achieved through hydrogen-bonding (see section 3.1.1) and electrostatic interactions by means of using separate entities such as polymers or dendrimers to regulate the interparticle distance. The group of Rotello employed PAMAM dendrimers of different generations (0–4) to assemble gold NPs and control the separation distance between them (Fig. 20).[212] In this approach, direct control of interparticle separation was provided through the choice of dendrimer generation. Gold NPs were functionalized with carboxylic acid groups. Salt-bridge formation between the dendrimer amino groups and the NP peripheral carboxylic acid groups led to electrostatic self-assembly between the dendrimer and NP components resulting in well-controlled aggregates. Interparticle distance in the aggregates formed was quantified by using small angle X-ray scattering (SAXS). It was observed that the sharp Bragg reflections shifted towards lower angles (larger interparticle distances) as the dendrimer generation increased. Control of interparticle spacing also provided a method for systematically shifting the surface plasmon resonance (SPR) of the particles, therefore having functional control over the NP aggregates.[213] In addition, these dendrimer-mediated NP assemblies open the door to create tailored magnetic NP structures.[214]

4.1.5 Charge transfer-directed nanoparticle assembly. Electron transfer interactions involve the partial transfer of a single electron from one molecule to another, or between two localized sites in the same molecule. This section will be focused on charge transfer (CT) interactions, that occur between an electron-donor and an electron-acceptor, and furthermore on the π–π interactions, that hold molecules together due to a sharing of electrons of sp^2 orbitals.

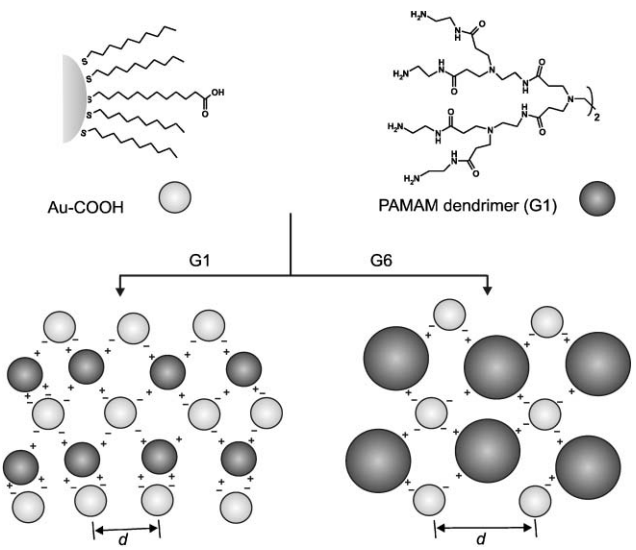

Fig. 20 Schematic representation of electrostatic self-assembly of carboxylic acid-terminated gold nanoparticles and PAMAM dendrimers, illustrating the control over average interparticle spacing, *d*, through dendrimer size.[212]

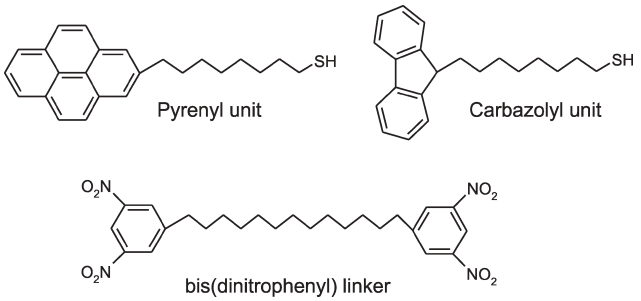

Fig. 21 Molecules used for charge transfer NP assembly.

The strategy employed by Chujo and co-workers to program self-assembly of colloidal gold NPs into macroscopic 3D aggregates involved the charge transfer interaction between pyrenyl units, as an electron donor, immobilized on the surface of the gold NPs and a divalent linker containing two dinitrophenyl units as an electron acceptor (Fig. 2.19).[215] The addition of the divalent linker to the pyrenyl-modified NP solution resulted in the formation of large, spherical aggregates with a diameter of 1 ± 0.7 μm, composed of individual gold NPs. The degree of colloidal association could be controlled by adjusting the concentration of the linker group in solution. Reversibility of the aggregated state was demonstrated by heating the solution to 50 °C and was found to be reproducible for several cycles. Recently, the same group described the formation of spherical aggregates induced by a charge transfer between the bis(dinitrophenyl) linker and 9-carbazolyl-modified gold NPs (Fig. 21).[216]

Photoinduced electron transfer and energy transfer in a number of donor–acceptor systems have been extensively studied with the aim of mimicking natural photosynthesis by converting the charge-separated state into chemical or electrical energy. This concept has been successfully demonstrated using fullerenes (C_{60}) for the construction of two- and three- dimensional nanoassemblies of photoactive molecules with colloidal metal particles. Brust and co-workers described the first NP assembly consisting of gold NPs and fullerenes.[217] In this study tetraoctylammonium bromide-stabilized gold particles in toluene were assembled into aggregates by the addition of C_{60} molecules. After the addition of the fullerenes, the ruby-colored solution slowly changed color to bluish violet, and it entirely precipitated after three weeks. TEM images showed the formation of strings of non-ordered 3D aggregates composed of gold nanoparticles. High resolution images showed that these particles were not in direct contact with each other but were apparently "glued" together by a shell of fullerene molecules.

With a focus on the preparation of organic solar cells, Fukumozi and co-workers reported the quaternary organization of porphyrin (donor) and fullerene (acceptor) dye units by clustering with gold NPs (Fig. 22).[218]

First, porphyrin–alkanethiolate gold NPs with well-defined sizes (8–9 nm) and spherical shape were prepared (secondary organization) from the primary components. Hereafter, these NPs formed complexes with fullerene molecules (tertiary organization), and they were clustered in an acetonitrile–toluene mixed solvent (quaternary organization). TEM

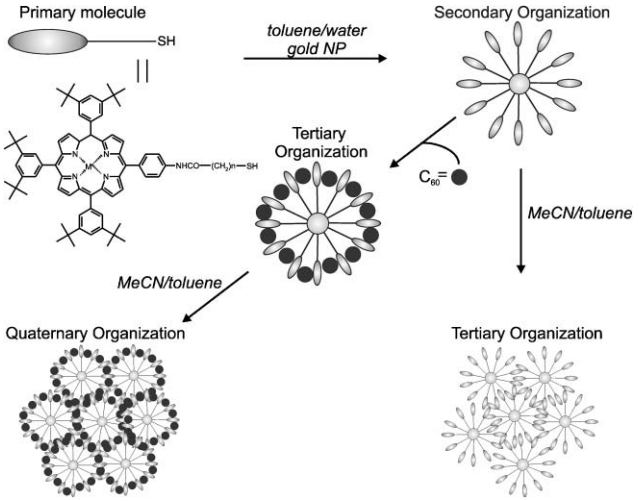

Fig. 22 Illustration of higher order organization of porphyrin and C_{60} units with gold NPs.

images of the quaternary organization displayed well-controlled size and shape of larger nanoclusters with a diameter of 300–400 nm. Control experiments of the porphyrin-modified NPs without C_{60} exhibited irregular and smaller clusters. From these experiments and from the diameter of the porphyrin-NPs in the quaternary organization (8–9 nm) the authors concluded that specific donor–acceptor interactions were needed to yield well-defined nanoclusters with an interpenetrating network (Fig. 22).

In a different strategy directed by π–π interactions, self-assembly of individual 2-carboxyterthiophene magnetic NPs was performed by Jin *et al.*[219] The individual NPs aggregated through weak π–π interactions forming spherical aggregates consisting of thousands of NPs, which could be easily redissolved by sonication. In order to analyze the magnetic characteristics of the aggregates, a superconducting quantum interference device (SQUID) magnetometer was employed. The field and temperature-dependent magnetization data for the aggregates showed that at lower temperatures (5 K) the magnetization of the aggregates increased and exhibited a symmetrical hysteresis loop, consistent with superparamagnetic behavior.

4.2 Biomolecule-directed nanoparticle assembly

The aggregation of NPs induced by specific biological interactions has attracted huge interest in the assembly of nanoscale components into controlled and sophisticated nanostructures in order to develop methods that mimic or exploit the recognition capabilities and interactions found in biology.[82,173,220] For the generation of biomolecule-crosslinked NPs, two types of complementary units should participate in the assembly process. Biomaterials utilized in the fabrication of such biomolecule–NP aggregates include complementary oligonucleotides, and protein pairs such as biotin–streptavidin and antigen–antibody. Besides the assembly into 3D nanostructures, the aggregation properties of biomolecule-modified NPs have been used in medicine for diagnostic assays,[83] such as immunoassays,[221] detection of polyvalent proteins,[222] and

detection of a virus in solution,[223] among others. This section is devoted to recent examples of these biological interactions for directing NP assembly.

4.2.1 Protein and carbohydrate-directed nanoparticle assembly. Proteins can be used to organize NPs into well-structured aggregates. The most frequently used protein–ligand system for such assemblies has been the biotin-streptavidin couple. The recognition between biotin and the homotetrameric streptavidin (SAv) is characterized by one of the highest stability constants known for noncovalent binding of a protein and a small ligand in aqueous solution, $K_a > 10^{14}$ M^{-1}.[224]

The first example of NP assembly based on protein binding was described by Connolly and Fitzmaurice in 1999.[225] Gold NPs were assembled in solution *via* two different routes. The first one consisted of the modification of gold NPs by chemisorption of a biotin-modified disulfide, followed by the addition of SAv; the second route involved the binding of the biotin adsorbate to SAv before the attachment onto the gold surface (Fig. 23).

The assembly of gold NPs was monitored by dynamic light scattering (DLS) showing a rapid increase in the average hydrodynamic radius upon addition of SAv accompanied by a color change of the solution from red to blue. TEM showed a homogeneous distribution of the unmodified gold NPs, while in the case of the biotin-modified NPs aggregated by addition of SAv, isolated particles were absent and larger aggregates with and interparticle distance of approximately 5 nm, corresponding to an interspersed SAv, were observed.

The SAv–biotin induced aggregation has also been used to assemble other systems like nanorods[226] and protein-encapsulated Fe_2O_3 NPs,[227] the latter with important applications in magnetic storage and nanoelectronic devices (Fig. 24).

Mann *et al.* have reported different strategies that involve the surface attachment of IgE or IgG antibodies to metal NPs followed by addition and subsequent crosslinking of a divalent antigen with appropriate double-headed functionalities.[228] The formation of specific antibody–antigen NP assemblies resulted in the formation of differently structured 3D network aggregates. Anti-dinitrophenyl (anti-DNP) IgE antibodies were chemisorbed onto 12 nm gold NPs and then bis-*N*-2,4-dinitrophenyloctamethylene diamine was added at a molar equivalence. No aggregation was observed but leaving the colloid dispersion at 4 °C gave a macroscopic purple precipitate, for which TEM revealed large disordered 3D

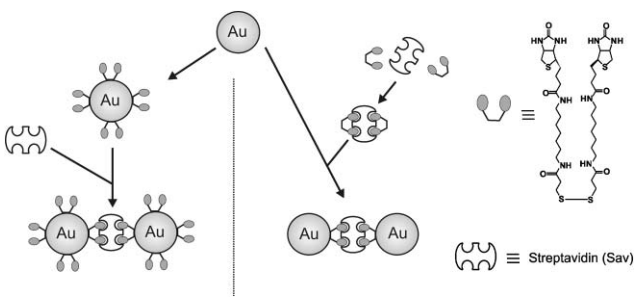

Fig. 23 Two routes for the aggregation of gold nanoparticles using streptavidin and a disulfide–biotin adsorbate.[225]

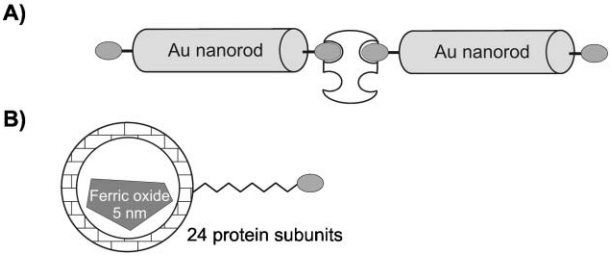

Fig. 24 (A) End-to-end assembly of biotin-functionalized gold nanorods that are crosslinked by SAv.[226] (B) Biotin-functionalized ferritin.[227]

networks of discrete gold NPs. Alternatively, two different antibody-modified NPs, anti-DNP IgE and anti-biotin IgG, were prepared. Equimolar mixtures of these antibody-coated NPs could be specifically aggregated by the addition of a synthetic ''Janus'' antigen, which consists of DNP and biotin haptens separated by a flexible linker. TEM showed structures of macroscopic filaments consisting of spatially separated gold NPs. Bimetallic nanoparticle aggregates comprising gold and silver were also obtained by using the DNP–biotin antigen biomolecular recognition.

Kotov and co-workers used a different antibody–antigen system to assemble luminescent CdTe NPs into ordered supramolecular aggregates.[229] Thiol-stabilized green- and red-emitting CdTe NPs were modified with bovine serum albumin (BSA) and the corresponding antibody (anti-BSA). When the IgG NPs (anti-BSA) with green luminescence were combined in a 1 : 1 molar ratio with BSA-labeled NPs with red-luminescence, an enhancement of the red-emission at 611 nm of the BSA NPs and a quenching of the green emission at 555 nm of the IgG NPs were observed. Apparently, the highly specific affinity of the antigen–antibody complex brought the NPs close enough to allow the resonance dipole–dipole coupling required for fluorescence resonance energy transfer (FRET). These results showed that well-organized assemblies of luminescent NPs could be obtained as well as an enhancement of the luminescent quantum yield in the bioconjugate, which is important for protein sensing.

Also carbohydrate–carbohydrate interactions have been used to drive NP assembly. Penadés and co-workers prepared oligosaccharide-functionalized gold NPs with a 3D polyvalent carbohydrate network,[230,231] and studied how carbohydrate–carbohydrate interactions can be used to guide the assembly of the gold clusters.[232] They prepared gold NPs functionalized with two biologically significant oligosaccharides: the lactose dissacharide (Lac–Au) and the trisaccharide Le^x antigen (Le^x–Au). In the presence of Ca^{2+} ions, specific carbohydrate-carbohydrate interactions between the Le^x antigen molecules in the Le^x–Au provoked the aggregation of the gold NPs, which could be reversed by the addition of EDTA. Addition of $CaCl_2$ to a Lac–Au NP solution did not cause any aggregation of the clusters. The authors also reported the functionalization of the gold NPs with fluorescein molecules together with Lac or Le^x oligosaccharides. These hybrid NPs showed self-organization onto a copper grid in a two-dimensional hexagonal structure defined by the gold centers.[232]

4.2.2 DNA-directed nanoparticle assembly. The specific recognition embedded in the sequence of the DNA double helix is being used more and more in nanoscience and nanotechnology, particularly as a versatile construction material specially due to its high specificity, and also its flexible length and the chemically programmable duplex structure.[83,233,234] The specificity of the adenine–thymine (A–T) and guanine–cytosine (G–C) Watson–Crick hydrogen bonding allows the construction of ordered systems with predictable structure. During the last few years, it has been demonstrated that one can use DNA to control the assembly of NPs in solution in the form of aggregates and small clusters and on substrates in the form of multilayered structures (paragraph 3.2). In all these nanomaterials, DNA is used mainly as a structuring element to drive the assembly of molecules that would not interact by themselves, or would do so in a disordered fashion.

DNA has also been used to develop a variety of biomolecule detection schemes based on the collective optical, catalytic, or electrical properties of DNA–NP conjugates.[235] Mirkin *et al.* reported a highly selective colorimetric detection technology for the detection of complementary DNA based on red-to-purple color changes resulting from the formation of a network of gold NPs.[235–237] The high sensitivity and selectivity of the DNA–NP assemblies for detection purposes often rival with fluorescent detection owing to the strong distance-dependent optical properties,[238] the melting temperatures,[239] and the electrical properties[240] of these DNA–NP assemblies. Moreover, Mirkin's colorimetric detection strategy has been expanded to the detection of other systems such as adenosine[241] and metal ions,[242] among others.

DNA has been extensively used as a building block for assembling NPs into network aggregates. The groups of Mirkin,[243,244] Alivisatos,[245] and Brust[246] have provided examples where oligonucleotides were used to order aggregates of gold NPs in solution. Mirkin and co-workers have developed many techniques for arranging NPs exploiting the code of oligonucleotides that are attached to them. The first strategy consisted of the introduction of a single-strand DNA to a solution of NPs modified with partially complementary DNA, where the single-strand DNA served as the ''glue'' to assemble the DNA NPs but only if the two halves were complementary to the DNA anchored on the NPs.[243] This approach has also helped them to assembly binary network materials comprising of two differently sized, DNA-functionalized NPs.[244] The structural characterization of such assemblies was performed with SAXS. In this study, issues like particle spacing depending upon different number of bases in the DNA interconnect, size of the NP building blocks and interparticle interactions have been discussed in detail.[247]

Alivisatos and co-workers have used an analogous approach to fabricate multiple trimer and tetramer architectures of DNA–gold NPs.[245,248] The authors reported a procedure where branched DNA scaffolds were hybridized in different positions to produce a three-armed dendritic structure comprised of one unique and two duplicate sequences. To generate well-defined assemblies, gold NPs functionalized with single strands of thiolated linear DNA were utilized. Following the same procedure, asymmetric structures were also produced in which 5 and 10 nm gold NPs were assembled on the DNA branched scaffolds. By using electrophoresis it was possible to isolate Au–DNA structures.[249]

A similar method of nanostructure manipulation was demonstrated by Brust and co-workers, in which biocatalyzed transformations of functionalized DNA assemblies were used to perform the controlled association of NPs and to provide stabilization of the aggregates.[246] 15 nm gold NPs were modified with thiolated single-strand DNA. The DNA-modified NPs were then converted to the double-strand form by hybridization with the complementary single-strand DNA. A restriction enzyme was used to cleave the double strands on the particles at specific sites. This resulted in cohesive ends of single-strand DNA, which can bind by hybridization to complementary sequences present in the system resulting in the formation of weak and small aggregates. More stable, larger aggregates were obtained in a second ligation step (Fig. 25).

A similar strategy, using DNA as a structuring element, has been used to create ordered aggregates composed of other types of NPs. For example, Mann and co-workers have used DNA to induce the programmed assembly of gold NPs onto silica NPs.[250] The field of semiconductor quantum dots (QDs) passivated with DNA has been explored by Mirkin and co-workers.[251] Modification of QDs with single-strand DNA generated DNA-linked QD assemblies through specific binding between complementary DNA strands. Moreover, the versatility of the system allowed the construction of hybrid metal–semiconductor nanostructures composed of DNA-modified gold NPs and DNA-modified QDs.

Fitzmaurice *et al.* were able to control NP aggregation in solution by attachment of complementary protein–DNA conjugates.[252] Gold NPs were modified with disulfide–biotin derivatives that were able to recognize and bind selectively SAv–DNA conjugates, resulting in NP assembly. The driving force for the assembly was the formation of a DNA duplex between the two complementary DNA oligomers bound to the individual NPs. The advantage of this methodology is that the aggregation rate can be controlled by the addition of single-strand DNA oligomers to a dispersion of NPs protein–DNA conjugates. The single-strand DNA immediately formed

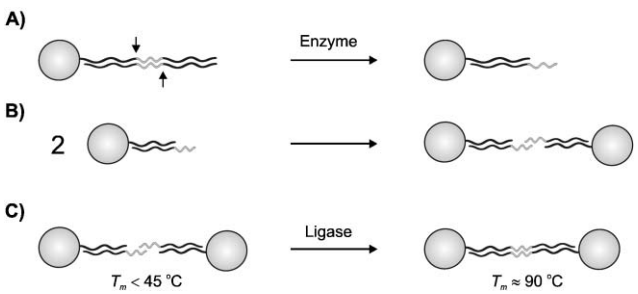

Fig. 25 Schematic representation of the method used by Brust and co-workers. (A) Gold NPs derivatized with double-strand DNA are treated with a restriction enzyme, which cleaves the DNA to yield cohesive ends. (B) Two cohesive ends hybridize, which leads to weak association of NPs. (C) The DNA backbones are covalently joined at the hybridized site by DNA ligase to yield a stable DNA double-strand link between the particles.[246]

duplexes with the immobilized DNA and the aggregation process was terminated (Fig. 26).

Moreover, the kinetics of the aggregation process could be changed by varying the salt and particle concentrations. The strong biotin–SAv interactions and the specific hybridization capabilities of DNA–SAv conjugates have also been used to organize gold NPs. Niemeyer and co-workers[253] modified 1.4 nm gold clusters with a single biotin group, where the biotin moiety was used to organize the nanoclusters into the tetrahedral superstructure, defined by the geometry of the biotin-binding sites. Furthermore, the nanocluster-loaded proteins self-assembled in the presence of the complementary single-strand DNA, therefore generating novel biometallic nanostructures. Introduction of a functional immunoglobulin, allowed the targeting of the biometallic nanostructures to specific tissues.

As explained in paragraph 2.2, proteins have been used to drive NP assemblies through specific interactions. However, since proteins and protein receptors can be functionalized with oligonucleotides, it is possible to immobilize such conjugates onto oligonucleotide-modified NPs and to generate new classes of hybrid particles exhibiting the high stability of the oligonucleotide-modified particles but at the same time having the molecular recognition properties of the protein. Taking advantage of that approach, Mirkin and co-workers designed three-building-block NP–protein assemblies: SAv complexed to four biotinylated oligonucleotides, oligonucleotide-modified gold NPs, and a linker oligonucleotide complementary to the other two groups. Addition of the three components and increasing the temperature of the solution to a few degrees below the melting temperature of the DNA interconnects resulted in the growth of micrometre-sized aggregates.[254]

Peptide nucleic acids (PNAs), which are DNA analogues in which the entire sugar–phosphate backbone is replaced by a polypeptide backbone, have also been used to drive NP aggregation.[255,256] The use of PNA complexes offers greater advantages for nanofabrication over the analogous DNA: (1) greater stability, and (2) greater mismatch sensitivity, which leads to an improved selectivity and makes them better suitable for biosensing.

5. Conclusions and outlook

In this review some examples of self-assembly at flat and nanoparticle surfaces have been discussed. Self-assembly has been shown to be a tool for the fabrication of 2D and 3D nanostructures. It has been demonstrated that it is possible to assemble molecules and nanometre-scale components, such as nanoparticles, polymers or biomolecules, into ordered arrays with dimensions larger than 100 nm. Such ordered arrays are difficult to achieve with a process other than self-assembly. Furthermore, the fundamental concept of self-assembly for the preparation of nanomaterials has been extended to integrate functional molecular components into ordered assemblies with well-defined architectures. The combination of such approaches with top-down methodologies will lead to well-defined functional 3D nanostructures and devices.

However, self-assembly as a nanofabrication tool is still in its infancy and a lot of effort is still required in order to make self-assembly a more valuable and versatile instrument for

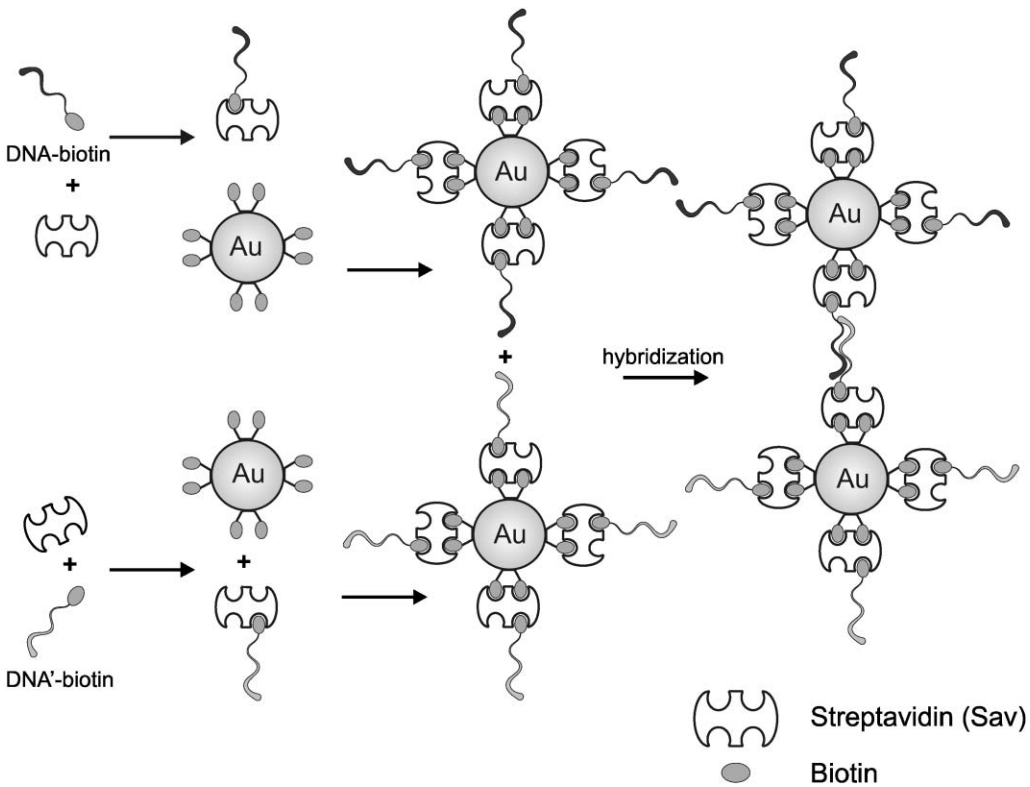

Fig. 26 Illustration of the biotin-modified NP assembly induced by the attachment of complementary SAv–DNA conjugates.[252]

nanofabrication schemes. Although self-assembly has been employed to produce nanostructures with a wide range of components, nonetheless the precise spatial positioning of components, the combination of many components within one structure, the preparation of arbitrary shapes and size, and the elimination of defects of such nanostructures are still open challenges that will need to be solved. Thus, self-assembly as a bottom-up chemical approach as yet requires the spatial confinement of conventional surface patterning techniques (top-down), such as soft lithography, in order to produce functional materials with long range order.

References

1 G. M. Whitesides and B. Grzybowski, *Science*, 2002, **295**, 2418–2421.
2 A. Ulman, *An Introduction to Ultrathin Organic Films: From Langmuir–Blodgett to Self-Assembly*, Academic Press, Boston, 1991.
3 A. Ulman, *Chem. Rev.*, 1996, **96**, 1533–1554.
4 C. Burda, X. B. Chen, R. Narayanan and M. A. El-Sayed, *Chem. Rev.*, 2005, **105**, 1025–1102.
5 S. Onclin, B. J. Ravoo and D. N. Reinhoudt, *Angew. Chem., Int. Ed.*, 2005, **44**, 6282–6304.
6 J. C. Love, L. A. Estroff, J. K. Kriebel, R. G. Nuzzo and G. M. Whitesides, *Chem. Rev.*, 2005, **105**, 1103–1170.
7 M. Mammen, S. K. Choi and G. M. Whitesides, *Angew. Chem., Int. Ed.*, 1998, **37**, 2755–2794.
8 A. Mulder, J. Huskens and D. N. Reinhoudt, *Org. Biomol. Chem.*, 2004, **2**, 3409–3424.
9 E. U. Thoden van Velzen, J. F. J. Engbersen, P. J. Delange, J. W. G. Mahy and D. N. Reinhoudt, *J. Am. Chem. Soc.*, 1995, **117**, 6853–6862.
10 H. Schönherr, G. J. Vancso, B. H. Huisman, F. C. J. M. van Veggel and D. N. Reinhoudt, *Langmuir*, 1997, **13**, 1567–1570.
11 B. H. Huisman, R. P. H. Kooyman, F. C. J. M. van Veggel and D. N. Reinhoudt, *Adv. Mater.*, 1996, **8**, 561–564.
12 A. Friggeri, F. C. J. M. van Veggel and D. N. Reinhoudt, *Chem. Eur. J.*, 1999, **5**, 3595–3602.
13 A. Friggeri, F. C. J. M. van Veggel, D. N. Reinhoudt and R. P. H. Kooyman, *Langmuir*, 1998, **14**, 5457–5463.
14 J. D. Faull and V. K. Gupta, *Langmuir*, 2002, **18**, 6584–6592.
15 J. D. Faull and V. K. Gupta, *Langmuir*, 2001, **17**, 1470–1476.
16 For comprehensive reviews on cyclodextrin chemistry see: V. T. D'Souza and K. B. Lipkowitz, *Chem. Rev.*, 1998, **98**(5).
17 A. Mulder, PhD thesis, University of Twente 2004 and references therein.
18 S. Onclin, A. Mulder, J. Huskens, B. J. Ravoo and D. N. Reinhoudt, *Langmuir*, 2004, **20**, 5460–5466.
19 M. T. Rojas, R. Königer, J. F. Stoddart and A. E. Kaifer, *J. Am. Chem. Soc.*, 1995, **117**, 336–343.
20 Y. Wang and A. E. Kaifer, *J. Phys. Chem. B*, 1998, **102**, 9922–9927.
21 A. Fragoso, E. Almirall, R. Cao, L. Echegoyen and R. González-Jonte, *Chem. Commun.*, 2004, 2230–2231.
22 D. Velic and G. Kohler, *Chem. Phys. Lett.*, 2003, **371**, 483–489.
23 Y. Maeda, T. Fukuda, H. Yamamoto and H. Kitano, *Langmuir*, 1997, **13**, 4187–4189.
24 H. Yamamoto, Y. Maeda and H. Kitano, *J. Phys. Chem. B*, 1997, **101**, 6855–6860.
25 M. R. de Jong, J. Huskens and D. N. Reinhoudt, *Chem. Eur. J.*, 2001, **7**, 4164–4170.
26 H. Endo, T. Nakaji-Hirabayashi, S. Morokoshi, M. Gemmei-Ide and H. Kitano, *Langmuir*, 2005, **21**, 1314–1321.
27 A. Michalke, A. Janshoff, C. Steinem, C. Henke, M. Sieber and H. J. Galla, *Anal. Chem.*, 1999, **71**, 2528–2533.
28 M. W. J. Beulen, J. Bügler, M. R. de Jong, B. Lammerink, J. Huskens, H. Schönherr, G. J. Vancso, B. A. Boukamp, H. Wieder, A. Offenhauser, W. Knoll, F. C. J. M. van Veggel and D. N. Reinhoudt, *Chem. Eur. J.*, 2000, **6**, 1176–1183.
29 T. Auletta, M. R. de Jong, A. Mulder, F. C. J. M. van Veggel, J. Huskens, D. N. Reinhoudt, S. Zou, S. Zapotoczny, H. Schönherr, G. J. Vancso and L. Kuipers, *J. Am. Chem. Soc.*, 2004, **126**, 1577–1584.
30 A. Mulder, T. Auletta, A. Sartori, S. Del Ciotto, A. Casnati, R. Ungaro, J. Huskens and D. N. Reinhoudt, *J. Am. Chem. Soc.*, 2004, **126**, 6627–6636.
31 T. Auletta, B. Dordi, A. Mulder, A. Sartori, S. Onclin, C. M. Bruinink, M. Péter, C. A. Nijhuis, H. Beijleveld, H. Schönherr, G. J. Vancso, A. Casnati, R. Ungaro, B. J. Ravoo, J. Huskens and D. N. Reinhoudt, *Angew. Chem., Int. Ed.*, 2004, **43**, 369–373.
32 A. Mulder, S. Onclin, M. Péter, J. P. Hoogenboom, H. Beijleveld, J. ter Maat, M. F. García-Parajó, B. J. Ravoo, J. Huskens, N. F. van Hulst and D. N. Reinhoudt, *Small*, 2005, **1**, 242–253.
33 J. Huskens, M. A. Deij and D. N. Reinhoudt, *Angew. Chem., Int. Ed.*, 2002, **41**, 4467–4471.
34 C. A. Nijhuis, F. Yu, W. Knoll, J. Huskens and D. N. Reinhoudt, *Langmuir*, 2005, **21**, 7866–7876.
35 J. Huskens, A. Mulder, T. Auletta, C. A. Nijhuis, M. J. W. Ludden and D. N. Reinhoudt, *J. Am. Chem. Soc.*, 2004, **126**, 6784–6797.
36 C. A. Nijhuis, J. Huskens and D. N. Reinhoudt, *J. Am. Chem. Soc.*, 2004, **126**, 12266–12267.
37 C. M. Bruinink, C. A. Nijhuis, M. Péter, B. Dordi, O. Crespo-Biel, T. Auletta, A. Mulder, H. Schönherr, G. J. Vancso, J. Huskens and D. N. Reinhoudt, *Chem. Eur. J.*, 2005, **11**, 3988–3996.
38 K. Motesharei and D. C. Myles, *J. Am. Chem. Soc.*, 1998, **120**, 7328–7336.
39 J. J. García-López, S. Zapotoczny, P. Timmerman, F. C. J. M. van Veggel, G. J. Vancso, M. Crego-Calama and D. N. Reinhoudt, *Chem. Commun.*, 2003, 352–353.
40 I. A. Banerjee, L. T. Yu and H. Matsui, *J. Am. Chem. Soc.*, 2003, **125**, 9542–9543.
41 Y. F. Chen, I. A. Banerjee, L. Yu, R. Djalali and H. Matsui, *Langmuir*, 2004, **20**, 8409–8413.
42 S. Samitsu, T. Shimomura, K. Ito and M. Hara, *Appl. Phys. Lett.*, 2004, **85**, 3875–3877.
43 T. B. Norsten, E. Jeoung, R. J. Thibault and V. M. Rotello, *Langmuir*, 2003, **19**, 7089–7093.
44 F. Corbellini, A. Mulder, A. Sartori, M. J. W. Ludden, A. Casnati, R. Ungaro, J. Huskens, M. Crego-Calama and D. N. Reinhoudt, *J. Am. Chem. Soc.*, 2004, **126**, 17050–17058.
45 Y. Ito, Y. S. Park and Y. Imanishi, *J. Am. Chem. Soc.*, 1997, **119**, 2739–2740.
46 C. S. Chen, M. Mrksich, S. Huang, G. M. Whitesides and D. E. Ingber, *Science*, 1997, **276**, 1425–1428.
47 K. Haupt and K. Mosbach, *Chem. Rev.*, 2000, **100**, 2495–2504.
48 G. P. Chen, T. Ushida and T. Tateishi, *Macromol. Biosci.*, 2002, **2**, 67–77.
49 S. J. Metallo, R. S. Kane, R. E. Holmlin and G. M. Whitesides, *J. Am. Chem. Soc.*, 2003, **125**, 4534–4540.
50 O. Crespo-Biel, M. Péter, C. M. Bruinink, B. J. Ravoo, D. N. Reinhoudt and J. Huskens, *Chem. Eur. J.*, 2005, **11**, 2426–2432.
51 H. Schönherr, M. W. J. Beulen, J. Bügler, J. Huskens, F. C. C. J. van Veggel, D. N. Reinhoudt and G. J. Vancso, *J. Am. Chem. Soc.*, 2000, **122**, 4963–4967.
52 T. B. Norsten, B. L. Frankamp and V. M. Rotello, *Nano Lett.*, 2002, **2**, 1345–1348.
53 A. Sanyal, T. B. Norsten, O. Uzun and V. M. Rotello, *Langmuir*, 2004, **20**, 5958–5964.
54 J. S. Park, G. S. Lee, Y. J. Lee, Y. S. Park and K. B. Yoon, *J. Am. Chem. Soc.*, 2002, **124**, 13366–13367.
55 T. Hatano, A. Ikeda, T. Akiyama, S. Yamada, M. Sano, Y. Kanekiyo and S. Shinkai, *J. Chem. Soc., Perkin Trans. 2*, 2000, **5**, 909–912.
56 B. H. Huisman, D. M. Rudkevich, F. C. J. M. van Veggel and D. N. Reinhoudt, *J. Am. Chem. Soc.*, 1996, **118**, 3523–3524.
57 S. A. Levi, P. Guatteri, F. C. J. M. van Veggel, G. J. Vancso, E. Dalcanale and D. N. Reinhoudt, *Angew. Chem., Int. Ed.*, 2001, **40**, 1892–1896.
58 E. Menozzi, R. Pinalli, E. A. Speets, B. J. Ravoo, E. Dalcanale and D. N. Reinhoudt, *Chem. Eur. J.*, 2004, **10**, 2199–2206.
59 J. H. Fendler, *Nanoparticles and Nanostructured Films: Preparation, Characterization and Applications*, Wiley-VCH, Weinheim, Germany, 1998.

60 A. N. Shipway, E. Katz and I. Willner, *ChemPhysChem*, 2000, **1**, 18–52.
61 D. Y. Wang and H. Möhwald, *J. Mater. Chem.*, 2004, **14**, 459–468.
62 T. Zhu, X. Y. Fu, T. Mu, J. Wang and Z. F. Liu, *Langmuir*, 1999, **15**, 5197–5199.
63 K. M. Chen, X. P. Jiang, L. C. Kimerling and P. T. Hammond, *Langmuir*, 2000, **16**, 7825–7834.
64 F. Auer, M. Scotti, A. Ulman, R. Jordan, B. Sellergren, J. Garno and G. Y. Liu, *Langmuir*, 2000, **16**, 7554–7557.
65 A. Gole, S. R. Sainkar and M. Sastry, *Chem. Mater.*, 2000, **12**, 1234–1239.
66 A. Gole, C. J. Orendorff and C. J. Murphy, *Langmuir*, 2004, **20**, 7117–7122.
67 R. R. Bhat, D. A. Fischer and J. Genzer, *Langmuir*, 2002, **18**, 5640–5643.
68 R. Maoz, S. R. Cohen and J. Sagiv, *Adv. Mater.*, 1999, **11**, 55–61.
69 R. Maoz, E. Frydman, S. R. Cohen and J. Sagiv, *Adv. Mater.*, 2000, **12**, 725–731.
70 S. Hoeppener, R. Maoz, S. R. Cohen, L. F. Chi, H. Fuchs and J. Sagiv, *Adv. Mater.*, 2002, **14**, 1036–1041.
71 S. T. Liu, R. Maoz, G. Schmid and J. Sagiv, *Nano Lett.*, 2002, **2**, 1055–1060.
72 S. T. Liu, R. Maoz and J. Sagiv, *Nano Lett.*, 2004, **4**, 845–851.
73 D. Wouters and U. S. Schubert, *J. Mater. Chem.*, 2005, **15**, 2353–2355.
74 S. Hoeppener and U. S. Schubert, *Small*, 2005, **1**, 628–632.
75 H. Tanaka, M. Mitsuishi and T. Miyashita, *Langmuir*, 2003, **19**, 3103–3105.
76 R. R. Bhat, J. Genzer, B. N. Chaney, H. W. Sugg and A. Liebmann-Vinson, *Nanotechnology*, 2003, **14**, 1145–1152.
77 P. Maury, M. Péter, V. Mahalingam, D. N. Reinhoudt and J. Huskens, *Adv. Funct. Mater.*, 2005, **15**, 451–457.
78 Z. Q. Peng, X. H. Qu and S. J. Dong, *Langmuir*, 2004, **20**, 5–10.
79 D. Ryan, L. Nagle and D. Fitzmaurice, *Nano Lett.*, 2004, **4**, 573–575.
80 V. Mahalingam, S. Onclin, M. Péter, B. J. Ravoo, J. Huskens and D. N. Reinhoudt, *Langmuir*, 2004, **20**, 11756–11762.
81 R. Zirbs, F. Kienberger, P. Hinterdorfer and W. H. Binder, *Langmuir*, 2005, **21**, 8414–8421.
82 E. Katz and I. Willner, *Angew. Chem., Int. Ed.*, 2004, **43**, 6042–6108.
83 N. L. Rosi and C. A. Mirkin, *Chem. Rev.*, 2005, **105**, 1547–1562.
84 C. M. Niemeyer, B. Ceyhan and P. Hazarika, *Angew. Chem., Int. Ed.*, 2003, **42**, 5766–5770.
85 C. M. Niemeyer, B. Ceyhan, M. Noyong and U. Simon, *Biochem. Biophys. Res. Commun.*, 2003, **311**, 995–999.
86 T. A. Taton, R. C. Mucic, C. A. Mirkin and R. L. Letsinger, *J. Am. Chem. Soc.*, 2000, **122**, 6305–6306.
87 C. M. Niemeyer and B. Ceyhan, *Angew. Chem., Int. Ed.*, 2001, **40**, 3685–3688.
88 J. D. Le, Y. Pinto, N. C. Seeman, K. Musier-Forsyth, T. A. Taton and R. A. Kiehl, *Nano Lett.*, 2004, **4**, 2343–2347.
89 J. K. N. Mbindyo, B. D. Reiss, B. R. Martin, C. D. Keating, M. J. Natan and T. E. Mallouk, *Adv. Mater.*, 2001, **13**, 249–254.
90 C. M. Niemeyer, B. Ceyhan, S. Gao, L. Chi, S. Peschel and U. Simon, *Colloid Polym. Sci.*, 2001, **279**, 68–72.
91 L. M. Demers, S. J. Park, T. A. Taton, Z. Li and C. A. Mirkin, *Angew. Chem., Int. Ed.*, 2001, **40**, 3071–3073.
92 L. M. Demers, D. S. Ginger, S. J. Park, Z. Li, S. W. Chung and C. A. Mirkin, *Science*, 2002, **296**, 1836–1838.
93 K. B. Lee, J. H. Lim and C. A. Mirkin, *J. Am. Chem. Soc.*, 2003, **125**, 5588–5589.
94 G. Decher, *Science*, 1997, **277**, 1232–1237.
95 G. Decher and J. B. Schlenoff, *Multilayer Thin Films*, Wiley, Weinheim, Germany, 2003.
96 P. T. Hammond, *Adv. Mater.*, 2004, **16**, 1271–1293.
97 W. B. Stockton and M. F. Rubner, *Macromolecules*, 1997, **30**, 2717–2725.
98 X. Q. Wang, K. Naka, H. Itoh, T. Uemura and Y. Chujo, *Macromolecules*, 2003, **36**, 533–535.
99 D. Li, Y. D. Jiang, Z. M. Wu, X. D. Chen and Y. R. Li, *Thin Solid Films*, 2000, **360**, 24–27.
100 A. Hatzor, T. Moav, H. Cohen, S. Matlis, J. Libman, A. Vaskevich, A. Shanzer and I. Rubinstein, *J. Am. Chem. Soc.*, 1998, **120**, 13469–13477.
101 T. Serizawa, S. Hashiguchi and M. Akashi, *Langmuir*, 1999, **15**, 5363–5368.
102 P. Kohli and G. J. Blanchard, *Langmuir*, 2000, **16**, 8518–8524.
103 J. Anzai and Y. Kobayashi, *Langmuir*, 2000, **16**, 2851–2856.
104 I. Suzuki, Y. Egawa, Y. Mizukawa, T. Hoshi and J. Anzai, *Chem. Commun.*, 2002, 164–165.
105 Y. L. Zhou, Z. Li, N. F. Hu, Y. H. Zeng and J. F. Rusling, *Langmuir*, 2002, **18**, 8573–8579.
106 Y. Shen, J. Y. Liu, J. G. Jiang, B. F. Liu and S. J. Dong, *J. Phys. Chem. B*, 2003, **107**, 9744–9748.
107 M. Olek, J. Ostrander, S. Jurga, H. Möhwald, N. Kotov, K. Kempa and M. Giersig, *Nano Lett.*, 2004, **4**, 1889–1895.
108 N. Dan, *Nano Lett.*, 2003, **3**, 823–827.
109 V. Panchagnula, C. V. Kumar and J. F. Rusling, *J. Am. Chem. Soc.*, 2002, **124**, 12515–12521.
110 A. P. R. Johnston, E. S. Read and F. Caruso, *Nano Lett.*, 2005, **5**, 953–956.
111 C. Picart, P. Lavalle, P. Hubert, F. J. G. Cuisinier, G. Decher, P. Schaaf and J. C. Voegel, *Langmuir*, 2001, **17**, 7414–7424.
112 S. J. Tian, J. Y. Liu, T. Zhu and W. Knoll, *Chem. Mater.*, 2004, **16**, 4103–4108.
113 P. J. Kulesza, M. Chojak, K. Karnicka, K. Miecznikowski, B. Palys, A. Lewera and A. Wieckowski, *Chem. Mater.*, 2004, **16**, 4128–4134.
114 N. Ferreyra, L. Coche-Guerente, J. Fatisson, M. L. Teijelo and P. Labbe, *Chem. Commun.*, 2003, 2056–2057.
115 P. J. G. Goulet, D. S. Dos Santos, R. A. Álvarez-Puebla, O. N. Oliveira and R. F. Aroca, *Langmuir*, 2005, **21**, 5576–5581.
116 K. Esumi, S. Akiyama and T. Yoshimura, *Langmuir*, 2003, **19**, 7679–7681.
117 T. Baum, D. Bethell, M. Brust and D. J. Schiffrin, *Langmuir*, 1999, **15**, 866–871.
118 M. D. Musick, C. D. Keating, L. A. Lyon, S. L. Botsko, D. J. Pena, W. D. Holliway, T. M. Mcevoy, J. N. Richardson and M. J. Natan, *Chem. Mater.*, 2000, **12**, 2869–2881.
119 F. P. Zamborini, J. F. Hicks and R. W. Murray, *J. Am. Chem. Soc.*, 2000, **122**, 4514–4515.
120 A. C. Templeton, F. P. Zamborini, W. P. Wuelfing and R. W. Murray, *Langmuir*, 2000, **16**, 6682–6688.
121 W. P. Welfing, F. P. Zamborini, A. C. Templeton, X. G. Wen, H. Yoon and R. W. Murray, *Chem. Mater.*, 2001, **13**, 87–95.
122 F. P. Zamborini, M. C. Leopold, J. F. Hicks, P. J. Kulesza, M. A. Malik and R. W. Murray, *J. Am. Chem. Soc.*, 2002, **124**, 8958–8964.
123 S. W. Chen, R. J. Pei, T. F. Zhao and D. J. Dyer, *J. Phys. Chem. B*, 2002, **106**, 1903–1908.
124 M. Wanunu, R. Popovitz-Biro, H. Cohen, A. Vaskevich and I. Rubinstein, *J. Am. Chem. Soc.*, 2005, **127**, 9207–9215.
125 O. Crespo-Biel, B. Dordi, D. N. Reinhoudt and J. Huskens, *J. Am. Chem. Soc.*, 2005, **127**, 7594–7600.
126 A. A. Mamedov, A. Belov, M. Giersig, N. N. Mamedova and N. A. Kotov, *J. Am. Chem. Soc.*, 2001, **123**, 7738–7739.
127 E. Donath, G. B. Sukhorukov, F. Caruso, S. A. Davis and H. Möhwald, *Angew. Chem., Int. Ed.*, 1998, **37**, 2202–2205.
128 G. B. Sukhorukov, E. Donath, S. Davis, H. Lichtenfeld, F. Caruso, V. I. Popov and H. Möhwald, *Polym. Adv. Technol.*, 1998, **9**, 759–767.
129 F. Caruso, R. A. Caruso and H. Möhwald, *Science*, 1998, **282**, 1111–1114.
130 G. Kaltenpoth, M. Himmelhaus, L. Slansky, F. Caruso and M. Grunze, *Adv. Mater.*, 2003, **15**, 1113–1118.
131 V. Salgueirino-Maceira, F. Caruso and L. M. Liz-Marzán, *J. Phys. Chem. B*, 2003, **107**, 10990–10994.
132 F. Caruso, R. A. Caruso and H. Möhwald, *Chem. Mater.*, 1999, **11**, 3309–3314.
133 F. G. Aliev, M. A. Correa-Duarte, A. Mamedov, J. W. Ostrander, M. Giersig, L. M. Liz-Marzán and N. A. Kotov, *Adv. Mater.*, 1999, **11**, 1006–1010.
134 A. J. Khopade and H. Möhwald, *Adv. Funct. Mater.*, 2005, **15**, 1088–1094.
135 F. Caruso and H. Möhwald, *J. Am. Chem. Soc.*, 1999, **121**, 6039–6046.

136 F. Caruso, *Adv. Mater.*, 2001, **13**, 11–22.
137 G. Schneider and G. Decher, *Nano Lett.*, 2004, **4**, 1833–1839.
138 A. M. Yu, Y. J. Wang, E. Barlow and F. Caruso, *Adv. Mater.*, 2005, **17**, 1737–1741.
139 A. Rogach, A. Susha, F. Caruso, G. Sukhorukov, A. Kornowski, S. Kershaw, H. Möhwald, A. Eychmuller and H. Weller, *Adv. Mater.*, 2000, **12**, 333–337.
140 X. Hong, J. Li, M. J. Wang, J. J. Xu, W. Guo, J. H. Li, Y. B. Bai and T. J. Li, *Chem. Mater.*, 2004, **16**, 4022–4027.
141 R. Georgieva, S. Moya, E. Donath and H. Baümler, *Langmuir*, 2004, **20**, 1895–1900.
142 G. Lu, S. Ai and J. B. Li, *Langmuir*, 2005, **21**, 1679–1682.
143 D. V. Volodkin, A. I. Petrov, M. Prevot and G. B. Sukhorukov, *Langmuir*, 2004, **20**, 3398–3406.
144 S. L. Clark, M. Montague and P. T. Hammond, *Supramol. Sci.*, 1997, **4**, 141–146.
145 S. L. Clark, M. F. Montague and P. T. Hammond, *Macromolecules*, 1997, **30**, 7237–7244.
146 X. P. Jiang, S. L. Clark and P. T. Hammond, *Adv. Mater.*, 2001, **13**, 1669–1673.
147 S. L. Clark and P. T. Hammond, *Adv. Mater.*, 1998, **10**, 1515–1519.
148 A. Pallandre, K. Glinel, A. M. Jonas and B. Nysten, *Nano Lett.*, 2004, **4**, 365–371.
149 F. Shi, B. Dong, D. L. Qiu, J. Q. Sun, T. Wu and X. Zhang, *Adv. Mater.*, 2002, **14**, 805–809.
150 Q. Li, J. H. Ouyang, J. Y. Chen, X. S. Zhao and W. X. Cao, *J. Polym. Sci., Part A: Polym. Chem.*, 2002, **40**, 222–228.
151 F. Shi, Z. Q. Wang, N. Zhao and X. Zhang, *Langmuir*, 2005, **21**, 1599–1602.
152 C. H. Lu, N. Z. Wu, F. Wei, X. S. Zhao, X. M. Jiao, J. Xu, C. Q. Luo and W. X. Cao, *Adv. Funct. Mater.*, 2003, **13**, 548–552.
153 T. B. Cao, F. Wei, X. M. Jiao, J. Y. Chen, W. Liao, X. Zhao and W. X. Cao, *Langmuir*, 2003, **19**, 8127–8129.
154 F. Hua, T. H. Cui and Y. Lvov, *Langmuir*, 2002, **18**, 6712–6715.
155 F. Hua, J. Shi, Y. Lvov and T. Cui, *Nano Lett.*, 2002, **2**, 1219–1222.
156 J. Park and P. T. Hammond, *Adv. Mater.*, 2004, **16**, 520–525.
157 E. Menard, L. Bilhaut, J. Zaumseil and J. A. Rogers, *Langmuir*, 2004, **20**, 6871–6878.
158 O. Crespo-Biel, B. Dordi, P. Maury, M. Péter, D. N. Reinhoudt and J. Huskens, *Chem. Mater.*, 2006, **18**, 2545–2551.
159 P. Maury, O. Crespo-Biel, M. Péter, D. N. Reinhoudt and J. Huskens, *MRS Symp. Proc.*, 2006, **901E0901-Rb12-01.1-9.**
160 X. P. Jiang, H. P. Zheng, S. Gourdin and P. T. Hammond, *Langmuir*, 2002, **18**, 2607–2615.
161 H. P. Zheng, M. F. Rubner and P. T. Hammond, *Langmuir*, 2002, **18**, 4505–4510.
162 H. P. Zheng, I. Lee, M. F. Rubner and P. T. Hammond, *Adv. Mater.*, 2002, **14**, 569–572.
163 I. Lee, H. P. Zheng, M. F. Rubner and P. T. Hammond, *Adv. Mater.*, 2002, **14**, 572–577.
164 H. Kim, J. Doh, D. J. Irvine, R. E. Cohen and P. T. Hammond, *Biomacromolecules*, 2004, **5**, 822–827.
165 H. P. Zheng, M. C. Berg, M. F. Rubner and P. T. Hammond, *Langmuir*, 2004, **20**, 7215–7222.
166 J. Feng, B. Wang, C. Y. Gao and J. C. Shen, *Adv. Mater.*, 2004, **16**, 1940–1944.
167 I. S. Lee, P. T. Hammond and M. F. Rubner, *Chem. Mater.*, 2003, **15**, 4583–4589.
168 A. C. Templeton, M. P. Wuelfing and R. W. Murray, *Acc. Chem. Res.*, 2000, **33**, 27–36.
169 R. Shenhar and V. M. Rotello, *Acc. Chem. Res.*, 2003, **36**, 549–561.
170 M. C. Daniel and D. Astruc, *Chem. Rev.*, 2004, **104**, 293–346.
171 T. Trindade, P. O'Brien and N. L. Pickett, *Chem. Mater.*, 2001, **13**, 3843–3858.
172 F. Raimondi, G. G. Scherer, R. Kotz and A. Wokaun, *Angew. Chem., Int. Ed.*, 2005, **44**, 2190–2209.
173 C. M. Niemeyer, *Angew. Chem., Int. Ed.*, 2001, **40**, 4128–4158.
174 Z. Y. Tang and N. A. Kotov, *Adv. Mater.*, 2005, **17**, 951–962.
175 D. Aherne, S. N. Rao and D. Fitzmaurice, *J. Phys. Chem. B*, 1999, **103**, 1821–1825.
176 A. K. Boal, F. Ilhan, J. E. Derouchey, T. Thurn-Albrecht, T. P. Russell and V. M. Rotello, *Nature*, 2000, **404**, 746–748.
177 R. Shenhar, T. B. Norsten and V. M. Rotello, *Adv. Mater.*, 2005, **17**, 657–669.
178 R. Deans, F. Ilhan and V. M. Rotello, *Macromolecules*, 1999, **32**, 4956–4960.
179 B. L. Frankamp, O. Uzun, F. Ilhan, A. K. Boal and V. M. Rotello, *J. Am. Chem. Soc.*, 2002, **124**, 892–893.
180 J. B. Carroll, B. L. Frankamp and V. M. Rotello, *Chem. Commun.*, 2002, 1892–1893.
181 A. K. Boal, B. L. Frankamp, O. Uzun, M. T. Tuominen and V. M. Rotello, *Chem. Mater.*, 2004, **16**, 3252–3256.
182 W. X. Zheng, M. M. Maye, F. L. Leibowitz and C. J. Zhong, *Anal. Chem.*, 2000, **72**, 2190–2199.
183 A. K. Boal and V. M. Rotello, *Langmuir*, 2000, **16**, 9527–9532.
184 S. Fullam, S. N. Rao and D. Fitzmaurice, *J. Phys. Chem. B*, 2000, **104**, 6164–6173.
185 J. Álvarez, J. Liu, E. Román and A. E. Kaifer, *Chem. Commun.*, 2000, 1151–1152.
186 J. Liu, J. Álvarez, W. Ong, E. Román and A. E. Kaifer, *Langmuir*, 2001, **17**, 6762–6764.
187 L. Strimbu, J. Liu and A. E. Kaifer, *Langmuir*, 2003, **19**, 483–485.
188 J. Liu, W. Ong, A. E. Kaifer and C. Peinador, *Langmuir*, 2002, **18**, 5981–5983.
189 J. Liu, S. Mendoza, E. Román, M. J. Lynn, R. L. Xu and A. E. Kaifer, *J. Am. Chem. Soc.*, 1999, **121**, 4304–4305.
190 J. Liu, J. Álvarez, W. Ong and A. E. Kaifer, *Nano Lett.*, 2001, **1**, 57–60.
191 O. Crespo-Biel, A. Jukvić, M. Karlsson, D. N. Reinhoudt and J. Huskens, *Isr. J. Chem.*, 2005, **45**, 353–362.
192 D. Fitzmaurice, S. N. Rao, J. A. Preece, J. F. Stoddart, S. Wenger and N. Zaccheroni, *Angew. Chem., Int. Ed.*, 1999, **38**, 1147–1150.
193 D. Ryan, S. N. Rao, H. Rensmo, D. Fitzmaurice, J. A. Preece, S. Wenger, J. F. Stoddart and N. Zaccheroni, *J. Am. Chem. Soc.*, 2000, **122**, 6252–6257.
194 D. Ryan, L. Nagle, H. Rensmo and D. Fitzmaurice, *J. Phys. Chem. B*, 2002, **106**, 5371–5377.
195 S. Leininger, B. Olenyuk and P. J. Stang, *Chem. Rev.*, 2000, **100**, 853–907.
196 Y. J. Kim, R. C. Johnson and J. T. Hupp, *Nano Lett.*, 2001, **1**, 165–167.
197 S. O. Obare, R. E. Hollowell and C. J. Murphy, *Langmuir*, 2002, **18**, 10407–10410.
198 S. Y. Lin, S. W. Liu, C. M. Lin and C. H. Chen, *Anal. Chem.*, 2002, **74**, 330–335.
199 T. H. Galow, A. K. Boal and V. M. Rotello, *Adv. Mater.*, 2000, **12**, 576–579.
200 A. K. Boal, T. H. Galow, F. Ilhan and V. M. Rotello, *Adv. Funct. Mater.*, 2001, **11**, 461–465.
201 J. Kolny, A. Kornowski and H. Weller, *Nano Lett.*, 2002, **2**, 361–364.
202 J. B. Carroll, B. L. Frankamp, S. Srivastava and V. M. Rotello, *J. Mater. Chem.*, 2004, **14**, 690–694.
203 X. Q. Wang, K. Naka, H. Itoh and Y. Chujo, *Chem. Lett.*, 2004, **33**, 216–217.
204 Z. Y. Zhong, S. Patskovskyy, P. Bouvrette, J. H. T. Luong and A. Gedanken, *J. Phys. Chem. B*, 2004, **108**, 4046–4052.
205 Z. Y. Zhong, A. S. Subramanian, J. Highfield, K. Carpenter and A. Gedanken, *Chem. Eur. J.*, 2005, **11**, 1473–1478.
206 Z. Y. Zhong, J. Z. Luo, T. P. Ang, J. Highfield, J. Y. Lin and A. Gedanken, *J. Phys. Chem. B*, 2004, **108**, 18119–18123.
207 P. R. Selvakannan, S. Mandal, S. Phadtare, R. Pasricha and M. Sastry, *Langmuir*, 2003, **19**, 3545–3549.
208 H. Hiramatsu and F. E. Osterloh, *Langmuir*, 2003, **19**, 7003–7011.
209 A. N. Shipway, M. Lahav, R. Gabai and I. Willner, *Langmuir*, 2000, **16**, 8789–8795.
210 E. Adachi, *Langmuir*, 2000, **16**, 6460–6463.
211 C. B. Murray, C. R. Kagan and M. G. Bawendi, *Annu. Rev. Mater. Sci.*, 2000, **30**, 545–610.
212 B. L. Frankamp, A. K. Boal and V. M. Rotello, *J. Am. Chem. Soc.*, 2002, **124**, 15146–15147.
213 S. Srivastava, B. L. Frankamp and V. M. Rotello, *Chem. Mater.*, 2005, **17**, 487–490.
214 B. L. Frankamp, A. K. Boal, M. T. Tuominen and V. M. Rotello, *J. Am. Chem. Soc.*, 2005, **127**, 9731–9735.
215 K. Naka, H. Itoh and Y. Chujo, *Langmuir*, 2003, **19**, 5496–5501.

216 K. Naka, H. Itoh and Y. Chujo, *Bull. Chem. Soc. Jpn.*, 2005, **78**, 501–505.
217 M. Brust, C. J. Kiely, D. Bethell and D. J. Schiffrin, *J. Am. Chem. Soc.*, 1998, **120**, 12367–12368.
218 T. Hasobe, H. Imahori, P. V. Kamat and S. Fukuzumi, *J. Am. Chem. Soc.*, 2003, **125**, 14962–14963.
219 J. Jin, T. Iyoda, C. S. Cao, Y. L. Song, L. Jiang, T. J. Li and D. Ben Zhu, *Angew. Chem., Int. Ed.*, 2001, **40**, 2135–2138.
220 S. Mann, W. Shenton, M. Li, S. Connolly and D. Fitzmaurice, *Adv. Mater.*, 2000, **12**, 147–150.
221 L. R. Hirsch, J. B. Jackson, A. Lee, N. J. Halas and J. West, *Anal. Chem.*, 2003, **75**, 2377–2381.
222 J. M. Nam, S. J. Park and C. A. Mirkin, *J. Am. Chem. Soc.*, 2002, **124**, 3820–3821.
223 J. M. Perez, F. J. Simeone, Y. Saeki, L. Josephson and R. Weissleder, *J. Am. Chem. Soc.*, 2003, **125**, 10192–10193.
224 P. C. Weber, D. H. Ohlendorf, J. J. Wendoloski and F. R. Salemme, *Science*, 1989, **243**, 85–88.
225 S. Connolly and D. Fitzmaurice, *Adv. Mater.*, 1999, **11**, 1202–1205.
226 K. K. Caswell, J. N. Wilson, U. H. F. Bunz and C. J. Murphy, *J. Am. Chem. Soc.*, 2003, **125**, 13914–13915.
227 M. Li, K. K. W. Wong and S. Mann, *Chem. Mater.*, 1999, **11**, 23–26.
228 W. Shenton, S. A. Davis and S. Mann, *Adv. Mater.*, 1999, **11**, 449–452.
229 S. P. Wang, N. Mamedova, N. A. Kotov, W. Chen and J. Studer, *Nano Lett.*, 2002, **2**, 817–822.
230 J. M. de La Fuente, A. G. Barrientos, T. C. Rojas, J. Rojo, J. Canada, A. Fernández and S. Penadés, *Angew. Chem., Int. Ed.*, 2001, **40**, 2257–2261.
231 A. G. Barrientos, J. M. de La Fuente, T. C. Rojas, A. Fernández and S. Penadés, *Chem. Eur. J.*, 2003, **9**, 1909–1921.
232 T. C. Rojas, J. M. de La Fuente, A. G. Barrientos, S. Penadés, L. Ponsonnet and A. Fernández, *Adv. Mater.*, 2002, **14**, 585–588.
233 B. Samori and G. Zuccheri, *Angew. Chem., Int. Ed.*, 2005, **44**, 1166–1181.
234 J. J. Storhoff and C. A. Mirkin, *Chem. Rev.*, 1999, **99**, 1849–1862.
235 R. Elghanian, J. J. Storhoff, R. C. Mucic, R. L. Letsinger and C. A. Mirkin, *Science*, 1997, **277**, 1078–1081.
236 J. J. Storhoff, R. Elghanian, R. C. Mucic, C. A. Mirkin and R. L. Letsinger, *J. Am. Chem. Soc.*, 1998, **120**, 1959–1964.
237 R. A. Reynolds, C. A. Mirkin and R. L. Letsinger, *J. Am. Chem. Soc.*, 2000, **122**, 3795–3796.
238 J. J. Storhoff, A. A. Lazarides, R. C. Mucic, C. A. Mirkin, R. L. Letsinger and G. C. Schatz, *J. Am. Chem. Soc.*, 2000, **122**, 4640–4650.
239 R. C. Jin, G. S. Wu, Z. Li, C. A. Mirkin and G. C. Schatz, *J. Am. Chem. Soc.*, 2003, **125**, 1643–1654.
240 S. J. Park, A. A. Lazarides, C. A. Mirkin, P. W. Brazis, C. R. Kannewurf and R. L. Letsinger, *Angew. Chem., Int. Ed.*, 2000, **39**, 3845–3848.
241 J. W. Liu and Y. Lu, *Anal. Chem.*, 2004, **76**, 1627–1632.
242 J. W. Liu and Y. Lu, *J. Am. Chem. Soc.*, 2003, **125**, 6642–6643.
243 C. A. Mirkin, R. L. Letsinger, R. C. Mucic and J. J. Storhoff, *Nature*, 1996, **382**, 607–609.
244 R. C. Mucic, J. J. Storhoff, C. A. Mirkin and R. L. Letsinger, *J. Am. Chem. Soc.*, 1998, **120**, 12674–12675.
245 S. A. Claridge, S. L. Goh, J. M. J. Frechet, S. C. Williams, C. M. Micheel and A. P. Alivisatos, *Chem. Mater.*, 2005, **17**, 1628–1635.
246 A. G. Kanaras, Z. X. Wang, A. D. Bates, R. Cosstick and M. Brust, *Angew. Chem., Int. Ed.*, 2003, **42**, 191–194.
247 S. J. Park, A. A. Lazarides, J. J. Storhoff, L. Pesce and C. A. Mirkin, *J. Phys. Chem. B*, 2004, **108**, 12375–12380.
248 A. P. Alivisatos, K. P. Johnsson, X. G. Peng, T. E. Wilson, C. J. Loweth, M. P. Bruchez and P. G. Schultz, *Nature*, 1996, **382**, 609–611.
249 D. Zanchet, C. M. Micheel, W. J. Parak, D. Gerion, S. C. Williams and A. P. Alivisatos, *J. Phys. Chem. B*, 2002, **106**, 11758–11763.
250 S. Sadasivan, E. Dujardin, M. Li, C. J. Johnson and S. Mann, *Small*, 2005, **1**, 103–106.
251 G. P. Mitchell, C. A. Mirkin and R. L. Letsinger, *J. Am. Chem. Soc.*, 1999, **121**, 8122–8123.
252 S. Cobbe, S. Connolly, D. Ryan, L. Nagle, R. Eritja and D. Fitzmaurice, *J. Phys. Chem. B*, 2003, **107**, 470–477.
253 C. M. Niemeyer, W. Burger and J. Peplies, *Angew. Chem., Int. Ed.*, 1998, **37**, 2265–2268.
254 S. J. Park, A. A. Lazarides, C. A. Mirkin and R. L. Letsinger, *Angew. Chem., Int. Ed.*, 2001, **40**, 2909–2912.
255 R. Chakrabarti and A. M. Klibanov, *J. Am. Chem. Soc.*, 2003, **125**, 12531–12540.
256 R. Levy, N. T. K. Thanh, R. C. Doty, I. Hussain, R. J. Nichols, D. J. Schiffrin, M. Brust and D. G. Fernig, *J. Am. Chem. Soc.*, 2004, **126**, 10076–10084.